

Copyright 2015 Abigail Esenam Asangba

MICROBIAL PHYLOGENETIC DIVERSITY PRESERVED IN FACIES-SPECIFIC  
MODERN, RECENT, HOLOCENE AND PLEISTOCENE HOT-SPRING TRAVERTINE  
DEPOSITS OF YELLOWSTONE AND TURKEY

BY

ABIGAIL ESENAM ASANGBA

THESIS

Submitted in partial fulfillment of the requirements  
for the degree of Master of Science in Geology  
in the Graduate College of the  
University of Illinois at Urbana-Champaign, 2015

Urbana, Illinois

Advisor:

Professor Bruce W. Fouke

## ABSTRACT

A systematic evaluation has been undertaken of the mechanisms and products of microbial community preservation within modern-to-ancient terrestrial hot-spring calcium carbonate ( $\text{CaCO}_3$ ) limestone deposits called *travertine*. Microbial 16S rRNA gene sequences preserved within Modern travertine deposited within the Proximal Slope Facies (PSF) at Mammoth Hot Springs (MHS), Yellowstone National Park, has been directly compared with analogous Holocene-Late Pleistocene PSF travertine at Gardiner, Montana, and Middle Pleistocene PSF travertine in Denizli, Turkey.

Analyses have included: (1) Modern microbial communities inhabiting the PSF of an actively depositing travertine hot-spring system (water, microbial mats, travertine) at MHS (0 YBP Modern travertine, Angel Terrace, Spring AT-1); (2) 9 YBP Modern PSF travertine (Angel Terrace, Spring AT-2; MHS); (2) ~100 YBP Recent travertine (New Highland Terrace, MHS); (3) ~4,000 YBP Holocene travertine (USGS Y-10 Core); (3) ~30,000 YBP Late Pleistocene travertine (Gardiner Quarry); and (4) ~1.1 Ma YBP Middle Pleistocene travertine (all of the Mammoth Hot Springs (YNP) and (Cakmak Quarry, Turkey). Genomic DNA entombed during rapid (up to 5 mm/day) travertine deposition and preserved within  $\text{CaCO}_3$  fluid inclusions and between crystals, was extracted via bulk rock drilling under sterile clean room conditions.

Pooled 16S rRNA gene sequence libraries were constructed via polymerase chain reactions (PCRs), terminal-restriction fragment length polymorphisms (T-RFLP), and MiSeq amplicon sequencing. Blast searches using multiple web-based bioinformatics tools identified over 400 operational taxonomic units (OTUs) affiliated with a total of 19 phyla (16 phyla and 3 candidate

phyla) within the Domain Bacteria. Previous analyses of the living microbial communities inhabiting modern active PSF depositional environments at MHS have provided a baseline with which to compare the ancient travertine analyses. Combined results from both MHS and Denizli indicate that only 3 of 19 phyla were detected in PSF travertine samples of all ages. Increasing depositional age of the travertine deposits was associated with increasing extents of post-depositional water-rock geochemical alteration (*diagenesis*). Microbial community structure shifted across this spatial and temporal transect from being dominated by Cyanobacteria and Proteobacteria in the Modern and Recent, to dominance by Firmicutes in the Holocene and Pleistocene. This is not unexpected, as endospores of Firmicutes are known to be resistant and also persist under harsh environmental conditions and therefore show higher relative abundance in ancient samples in comparison to modern samples. Preliminary blast search results imply that libraries from all PSF travertine samples of all ages contain photoautotrophic, chemoautotrophic and heterotrophic metabolic activities, which is likely the result of both original hot-spring depositional processes and secondary diagenetic alteration.

*To my fiancé, mum and siblings*

## ACKNOWLEDGEMENTS

This project would not have been possible without the support of many people.

Many thanks to my advisor, Dr. Bruce W. Fouke, who read my numerous revisions and helped, make some sense of the confusion. I also want extend my appreciation to Dr. Robert Sanford who offered guidance and support. My appreciation also goes to all Fouke Lab members especially Yiran Dong, Laura DeMott, Erin Murphy, and Ryanne Ardisana who contributed in diverse ways to the completion of this work. I also extend appreciation to Shane Butler (past member of the Fouke Lab) who collected some of the samples used in this study. Last but not the least, I would also like to thank Eva De Boever and Anneleen Foubert who provided the Turkey samples for this study and also for their guidance and support.

Thanks to the University of Illinois Graduate College for awarding me a graduate research assistantship for my Master's program. My appreciation also goes to the Dutch Oil Company, Total E&P and the Department of Geology, UIUC for providing me with the financial means to complete this project as well as paying my monthly stipend. My appreciation also goes to Marilyn Whalen and Lana Holben for their administrative assistance and moral support.

And finally, my appreciation goes to my fiancé, mum, siblings and numerous friends who helped me in diverse ways, always offering support and love.

## TABLE OF CONTENTS

CHAPTER 1: INTRODUCTION .....	1
CHAPTER 2: GEOBIOLOGICAL SETTING .....	6
CHAPTER 3: MATERIALS AND METHODS .....	12
CHAPTER 4: RESULTS .....	23
CHAPTER 5: DISCUSSION .....	29
CHAPTER 6: CONCLUSIONS .....	41
CHAPTER 7: FIGURES AND TABLES .....	43
REFERENCES .....	68

# CHAPTER 1

## INTRODUCTION

Phylogenetic analysis of 16S ribosomal RNA suggests that the earliest, most deeply rooted forms of microbial life were heat-loving (hyperthermophilic and thermophilic) bacteria that inhabited the early Earth (Woese 1987; Stetter, 1996). Abundant natural thermal environments still exist on earth and some have properties similar to the thermal environments on the early earth in which life possibly began (Canganella and Wiegel, 2014). These thermal environments include solfataric fields such as hot springs and submarine hydrothermal vents (Stetter et al., 1990; Canganella and Wiegel, 2014). Recent studies suggest that early Mars (> 3 Ga) by analogy to earth may have also had such suitable hydrothermal aqueous environments capable of harboring similar thermophilic microorganisms (Pollack et. al., 1987; Knoll, 2003; Villanueva et al., 2015). Russell and Hall (1997 and 1999) suggested that life would have emerged in medium enthalpy alkaline hot springs where ground waters already charged with hydrogen equilibrate with the Martian crust, meet the Martian hydrosphere. The evidence of this life may have been trapped and preserved in the carbonate and/or silica precipitates (Allen et al., 2000). This makes the study of life trapped and preserved in carbonate precipitated from hot springs very critical not only in understanding life on the early earth but also possible life on the early Mars and other planets.

Calcium carbonate (CaCO<sub>3</sub>) is deposited at extremely high rates (>2mm/day) in some classes of hot springs that harbor thermophilic microbes, creating limestone mineral deposits known as *travertine* (Fouke et al., 2000; Fouke et al., 2003; Fouke, 2011).



They are usually, characterized by high dissolved  $\text{Ca}^{2+}$  and other carbonate species (Pentecost 2005). The water chemistry directly related to temperature controls the extent to which microorganisms grow in these travertine deposits (Guo and Riding 1998; Fouke et al., 2000; Fouke et al., 2003; Zhang et al., 2004; Kandianis et al., 2008, Fouke, 2011). These microorganisms in turn influence the precipitation and deposition of travertine. Cyanobacteria and other phototrophs for instance are suggested to remove carbon dioxide from the water during photosynthesis increasing the likelihood of precipitation, and their cell surface constituents assist in the binding and nucleation of calcite (Golubic, 1973; (Pentecost and Bauld, 1988; Pentecost, 1990; Mann, 2001; Kandianis et al., 2008). These travertine deposits also share several features with stromatolites, which are known to be the earliest forms of life, including forming laminated structures and containing Cyanobacteria (Golubic and Focke, 1978, Chafetz and Folk, 1984; Pentecost 1990; Fouke et al., 2003; Fouke, 2011). This further makes travertine deposits very relevant environments in understanding life on the early earth.

The fossil record of the entombed and preserved early thermophilic microbial life in these hot spring travertine deposits, forms physical, chemical and biological “biomarkers” that include nucleic acids (DNA and RNA), lipids, isotopes, crystal shape, size, form and growth rate (Walter, 1996; Boschker and Middelburg, 2002; Kandianis et al., 2008; Fouke, 2011). The study of these biomarkers provides a means of determining the major extant and extinct microbial species inhabiting these extreme and complex ecosystems over time (Tunlid and White, 1992; Boschker and Middelburg, 2002; Fouke et al., 2003; Zhang et al., 2004; Vreeland et al. 2006; Fouke, 2011). A number of previous studies have identified physical biomarkers in the form of shrubs containing bacteria “clumps” and scattered intact cells from different locations including

Italy (Chafetz and Folk, 1984; Allen et al., 2000), East Africa (Casanova, 1986) and Mammoth Hot Springs, USA (Pentecost, 1990; Allen et al., 2000). It is therefore important to utilize other types of biomarkers (e.g. lipids and nucleic acids) when possible to further elucidate the composition and diversity of microbial communities entombed and preserved these travertine deposits.

It is however often extremely challenging to decipher true biotic “biomarkers” from similar crystallized fossil morphologies (shape, size and form), minerals and hydrocarbons formed by abiotic processes, as illustrated by the controversial interpretations of the putative biomarkers in calcites of the Martian meteorite ALH84001 (McKay et al., 1996). The presence of tens-of-nanometer-size magnetite ( $\text{Fe}_3\text{O}_4$ ) crystals found within carbonate spherules and their associated rims in the meteorite were similar both morphologically and chemically to magnetite particles produced by terrestrial magnetotactic bacteria and were therefore interpreted to be of biotic origin (McKay et al., 1996; Thomas-Keprta et al. 2000; Thomas-Keprta et al., 2001; Thomas-Keprta et al., 2002). Fouke et al., (2000) established a 5-fold travertine depositional facies model in the modern Mammoth Hot Springs, which has been consistently observed within the ancient hot spring travertine deposits as well (Butler, 2007; Fouke, 2011). These studies have shown that the depositional facies observed in the modern hot spring system have been preserved to a great extent in the ancient systems as well and can therefore be accurately tracked back in the geological record. Analyzing biomarkers in a depositional facies systems context therefore helps eliminate problems with determining if the biomarker of choice is biotic or abiotic since they can be tracked over time (Fouke et al., 2000; Fouke et al., 2003; Zhang et al., 2004; Bonheyo et al.,

2005; Kandianis et al., 2008; Fouke 2011). This study utilizes this facies model to track DNA biomarkers accurately into the geological record.

To the best of our knowledge, no culture-independent studies to elucidate the microbial community composition and diversity have been conducted to date on the modern-to-ancient travertine deposits. Compared to the abundant analyses of actively flowing modern hot springs and their associated microbial mats, relatively little is known about the microbial communities in the older travertine deposits. The current study was undertaken to develop and refine a new suite of biomarkers, which are composed of microbial biomolecules (DNA) preserved in bulk-rock sampled intra- and inter-crystalline  $\text{CaCO}_3$  crystals comprising travertine deposits. We used culture-independent DNA-based molecular phylogenetic methods to systematically study changes in microbial DNA as a biomarker, during precipitation, fossilization and diagenesis of travertine to reconstruct the phylogenetic and metabolic diversity of the microbial communities and their carbonate precipitating hot-spring environments. To achieve this goal, we hypothesized that microbial DNA is well preserved in modern-to-ancient travertine and can be analyzed to reconstruct the phylogenetic and metabolic diversities of the modern through ancient microbial communities. We compared modern-Holocene travertine deposited within the Proximal Slope Facies (PSF) at Mammoth Hot Springs (MHS), Yellowstone National Park, to analogous Holocene-Late Pleistocene proximal slope facies travertine at Gardiner, Montana, and Middle Pleistocene proximal slope facies travertine in Denizli, Turkey.

The study of ancient DNA enables us to study extinct species and also provides a means of tracking temporal changes directly in environmental samples. There are however a number of

potential difficulties in identifying the ancient microbial molecules in these samples including contamination from exogenous DNA, DNA damage, presence of PCR inhibitors and the absolute quantity of DNA (Willerslev and Cooper, 2005; Oskam et al., 2010). In the case of travertine there is the possibility of post-depositional (*diagenetic*) alteration of these molecular biomarkers from combined physical, chemical and biological processes, as well as contamination from present day microbial molecules (Hazen and Roeder 2001; Willerslev et al., 2004; Hebsgaard et al., 2005; Fouke, 2011).

Various degrees of diagenetic alterations observed in the ancient travertine deposits due to water-rock-interactions are capable of introducing new microbial populations and in the process remove some original populations. Petrographic and selective nucleic acids staining procedures are currently underway to determine the extent of contamination due to diagenesis. In order to avoid contamination introduced during analysis, all necessary sterile handling precautions were taken during sample collection from the field as well as during the molecular analysis in the laboratory under clean room conditions.

The change in microbial composition and diversity over time was determined in modern-to-ancient travertine samples used in the study. Results imply that unaltered microbial molecular biomarkers are preserved in, and can be extracted from, ancient hot-spring travertine deposits. This was made possible by the use of the travertine depositional facies model to track these biomarkers over geological time.

## CHAPTER 2

### GEOBIOLOGICAL SETTING

#### 2.1 Mammoth Hot Springs (MHS), Yellowstone National Park (YNP)

The MHS thermal complex in YNP is the second largest site in the world of active travertine deposition after Pamukkale, Turkey (Pentecost, 2005). MHS is located ~8 km south of the northern entrance of YNP and covers an area of ~4 km<sup>2</sup> with a maximum thickness of 75 m of travertine accumulation and therefore creates an excellent natural laboratory for this study (Fig. 1; Allen and Day, 1935; Bargar, 1978; Sturchio, 1990; Fouke, 2011). The underlying 3 km thick strata are composed of Paleozoic and Mesozoic conglomerates, sandstones, shales, and limestones deposited in marginal marine settings (Harris et al., 1997). The system consists of active modern springs, Holocene deposits from upper surface of MHS and the Y-10 Core as well as Pleistocene Gardiner samples which have been well studied (Bargar, 1978; Sturchio, 1990; Sturchio, 1992; Fouke et al., 2000; Fouke et al., 2003; Fouke, 2011).

Several modern travertine-precipitating hot springs are present at MHS and are preserved in their natural state due to long-term protection by the National Park Service (NPS). The source of the dissolved HCO<sub>3</sub><sup>-</sup> and Ca<sup>2+</sup> in the spring water (Ca-Na-HCO<sub>3</sub>-SO<sub>4</sub> type) is the underlying Pleistocene limestone deposited in marine settings (Sorey, 1991). Modern travertine precipitates actively and rapidly (>2mm/day) at the Angel Terrace (AT) Springs as a result of complex interplay of both biotic and abiotic processes (Friedman, 1970; Fouke et al., 2000, 2003; Kandianis et al., 2008; Veysey & Goldenfeld, 2008; Fouke, 2011). This rapid precipitation rates may help increase the probability of trapping and preserving evidence of life in the form of biomarkers (Pentecost, 2003; Fouke 2011). These biomarkers may be trapped by means of fluid

inclusions within travertine crystals (intra-crystal) or between crystals (inter-crystal) (Vreeland et al., 2006).

In addition, a suite of analogous ancient travertine deposits as old as 33,000 years before present (YBP) are accessible in the MHS. Recent travertine ( $\leq 100$  years BP) can be observed at the New Highland Terrace (NHT) of the MHS complex. Travertine near Bath Lake was cored (Y-10 Core) by United States Geological Survey (USGS) in 1967 to a depth of  $\sim 101$  m with travertine making up  $\sim 77$  m (Fig. 3, White et al., 1975; Sorey, 1991). Cretaceous siliciclastic sandstones and mudstones make up the rest of the depth of the core. Sturchio in 1992, using uranium series dating, reported ages from 0 - 8,000 YBP for the entire  $\sim 101$  m thick Y-10 Core. Twelve kilometers to the north of MHS just above Gardiner, Wyoming (Fig. 1) is a  $7\text{km}^2$  accumulation of older Holocene and Pleistocene travertine. Travertine deposits from the Gardiner quarries range from 11,000 to 33,000 YBP (Fouke 2011).

Extensive research on the physical, chemical and biological components of the MHS system have been previously well conducted, with respect to quantification of the travertine precipitation rates, crystalline fabrics, geochemistry and diagenetic alteration (Bargar, 1978; Sturchio, 1990; Sturchio, 1992; Fouke et al., 2000; Fouke et al., 2003; Kandianis et al., 2008; Fouke, 2011). Kandianis et al., in 2008 reported a direct microbial biomass influence on travertine precipitation and growth rate and crystalline structure in active travertine hot springs. Butler (2007) described the crystalline fabrics of the ancient travertine from the various facies and reported an extensive preservation of the apron and channel, pond, and proximal slope facies of the Gardiner travertine deposits.

These and many other previous studies make it possible to use MHS as a modern analog for understanding the ancient travertine deposits located at MHS and in the Gardiner Quarry. Of specific importance to this study, is the establishment of a systematic 5-fold travertine depositional facies model in the modern springs that has been consistently observed within the ancient hot-spring travertine deposits of the Y-10 core and Gardiner (Fouke et al., 2000; Butler et al., 2007; Fouke, 2011). This was based on water temperature, chemistry, mineralogy, physical structure, and travertine accumulation rates (Fig. 2). These facies include the vent (66–73°C), the apron and channel (60–70°C), the pond (39–62°C), the proximal slope (35–65°C), and the distal slope (28–44°C). The spring water erupts, cools and degasses CO<sub>2</sub> changing to the pH from ~6 to ~8 from the vent to distal slope facies. Travertine in each of these facies is composed of a distinct assemblage of aragonite needles and calcite crystals into characteristics larger-scale carbonate accumulations (Fouke et al., 2000). Mineralogy changes from mainly aragonite (Vent and Apron and Channel facies) to a mixture of aragonite and calcite (Pond and Proximal Slope facies) to calcite in the Distal Slope facies (Fouke et al., 2000).

Fouke et al. (2003) through facies-by-facies microbial molecular analyses of the modern MHS hot-spring systems reported a direct correlation between bacterial communities and established modern travertine depositional facies. Zhang et al., (2004) via the analyses of lipid biomarkers and carbon isotopes in microbial mats that encrust travertine deposits along the continuous drainage outflow system of Spring AT-1 also observed distinctly different compositions of phospholipid fatty acids (PLFA) and glycolipid fatty acids (GLFA) in each of the facies. These results suggest that travertine depositional facies, effectively predict bacterial community composition as well as the morphology and chemistry of travertine precipitation (Fouke et al.,

2003; Zhang et al., 2004; Fouke 2011). Having determined the microbial community and compositions present in the various facies in the modern system, these studies make it possible to track these biomarkers in the various facies in a time series manner over the geological time.

## 2.2 Cakmak quarry, Ballık Area, Denizli Basin, SW Turkey

The Denizli Basin of Turkey is the largest travertine-precipitating site on earth and has travertine occupying more than 100 km<sup>2</sup> in the basin with a thickness of up to 75 m (Ozkul et al., 2002; Kele et al., 2010; Ozkul et al., 2013). The Denizli graben located in the Western Anatolian Extensional Province of Turkey (Fig. 4A), bounded by normal faults along its northern and southern margins (Alçıçek et al., 2007; Van Noten et al., 2013; Ozkul et al., 2013). The system comprises of active travertine precipitating springs at Pamukkale and ancient travertine deposits located in the Denizli Basin of Turkey.

The modern travertine terraces of Pamukkale are located about 17 km north of the city of Denizli (Ozkul et al., 2013). A series of fault-guided carbon dioxide containing thermal springs precipitate travertine covering a length of almost 3 km (Pentecost et al., 1997; Ozkul et al., 2013). Travertine precipitation results from the escape of CO<sub>2</sub> from the bicarbonate-rich groundwater (Pentecost et al., 1997). The springs, which have been used for curing and spa purposes are currently strongly controlled, mainly for touristic (bathing) purposes with a possibility of the spring water being contaminated (Pentecost et al., 1997; Pamukkale travertine - UNESCO World Heritage).



Several studies have been previously completed covering the basic suite of physical, chemical and biological components of the Pamukkale modern hot spring system (Pentecost et al, 1997; Alçiçek et al., 2007; Kele et al., 2011; Özkul et al., 2013). The current spring waters at the Pamukkale site are of the Ca-Mg-SO<sub>4</sub>-HCO<sub>3</sub>-type and emerge at temperatures of about 57°C to 35°C and a pH of 6.0 to 7.4 that increases downstream up to 7.8 with a temperature decrease until 20°C (Kele et al., 2011; Özkul et al., 2013; Pentecost et al., 1997). Travertine δ<sup>13</sup>C values of the Denizli area travertine suggest a mixture of CO<sub>2</sub> sources with an important contribution of thermometamorphic (Paleozoic metamorphosed carbonates) and magmatic CO<sub>2</sub>, in addition to CO<sub>2</sub> derived from the degradation of organic matter (Claes et al., in press; Kele et al., 2011; Özkul et al., 2013). Oxygen stable isotopes and radiogenic Sr-isotopes indicate that carbonates of the thrust, Triassic Lycian nappes were flushed by and interacted with infiltrating meteoric waters, providing the Ca<sup>2+</sup> and HCO<sub>3</sub><sup>-</sup> source (Claes et al., *submitted*; El Desouky et al., 2014). Molecular analysis confined only to the modern Pamukkale travertine by Pentecost et al., (1997), revealed a microbial community composition dominated by phototrophs (Cyanobacteria, diatoms and Chlorophyceae).

The Ballik area located on the northern flank of the Denizli graben (SW Turkey) is part of an extensive system of modern-to-ancient travertine deposits scattered over a total area of about 10 – 14 km in width and 50 km in length (Ozkul et al., 2013). These travertine deposits are excavated along the graben edge and the lower thick domal Ballik area (Özkul et al., 2013; De Boever et al., *submitted*). The Cakmak quarry is one of the main quarries in the central domal Ballik travertine area and provides a suite of analogous ancient travertine deposits for comparative study. The travertine deposits are interlain by marls, conglomerates, sandstones and

mudstones. U-Th dating of travertine deposits throughout the Denizli Basin indicate that carbonate spring activity lasted for more than 600 ka (Özkul et al., 2013). Lebatard et al. (2014) recently found that travertine ages in the domal Ballik area might even reach up to 1.1 – 1.3 Ma.

Recent work by De Boever et al. (*submitted*) has shown that the modern 5-fold MHS travertine depositional facies model is directly applicable to interpreting the modern and ancient hot-spring travertine deposits of Pumakkale and the Denizli region. This allows the use of analogous travertine samples from these locations in a time series manner to track the changes in microbial community composition and diversity over geologic time. Using the facies model therefore, samples from these two locations were used in this study in a time series manner. Cretaceous and older-aged lacustrine and travertine deposits (analogous to those at MHS, Gardiner and the Denizli region) along the South Atlantic marginal basins of Brazil and Angola have been recently recognized as large-scale subsurface hydrocarbon reservoirs (Carminatti et al., 2008; Arbouille et al., 2013). Microbially influenced carbonates have thus become targets of extensive global oil and gas exploration activities. There is however little data available for the construction of facies models for these carbonate hydrocarbon reservoirs. The facies, fabric and mapping results from the Pleistocene travertine deposits of MHS, Gardiner and the Denizli region represent good analogs which can serve as scale link between the biotic-abiotic interactions observed at smaller scales and controls on large scale (reservoir) structures of travertine bodies (Fouke, 2011; De Boever et al., 2015 (*submitted*))

## CHAPTER 3

### MATERIALS AND METHODS

#### 3.1 Deposition, Stratigraphy, Chronology, and Field Collection of Travertine Samples

Travertine samples ranging in age from Modern, Holocene to middle Pleistocene exclusively from the Proximal Slope Facies (PSF) were analyzed in this study. With a temperature range of 35-65°C and pH range of 6.9-8.0, the PSF of the modern terraced hot-spring travertine environment (described in Fouke et al. 2000), is composed primarily of arcuate aragonite needle shrubs ( $\leq 100 \mu\text{m}$ ) and blocky prismatic calcite (50-100  $\mu\text{m}$ ) that create microterraces on the steep face of the terrace margins. Sampling has included: (1) active travertine (0 YBP, Angel Terrace Spring AT-1, MHS); (2) ~100 YBP Recent travertine (New Highland Terrace, MHS); (3) ~4,000 YBP Holocene travertine (USGS Y-10 Core); (3) ~30,000 YBP Late Pleistocene travertine (Gardiner Quarry); and (4) ~1.1 Ma YBP Middle Pleistocene travertine (all of the Mammoth Hot Springs (YNP) and (Cakmak Quarry, Turkey).

All ancient samples prior to collection were examined for morphological evidence of travertine depositional preservation (Fouke et al., 2000). This was done by careful field observation to determine facies best preserved and the PSF was one of the best-preserved facies observed. To minimize contamination, in all cases of sample collection, drill bits, scapula blades and spatula, were thoroughly cleaned and sterilized with HCl, 10% bleach, and 70% isopropyl alcohol before the fieldtrip and then before drilling or sample collection. Samples were stored immediately on ice sterile Whirlpak bags and sterile Falcon centrifuge tubes, and subsequently transferred into a Taylor-Wharton liquid nitrogen dry shipper (Taylor-Wharton, Theodore, AL) for transport back

to UIUC where they were stored at -80°C. Table 1 shows a summary of samples with their descriptions.

### 3.1.1 ~0 YBP Modern AT-1 Travertine sample

The 0 YBP modern travertine from AT-1 was collected, prepared and analyzed as reported in Fouke et al., (2003).

### 3.1.2 ~9 YBP Modern AT-2 Travertine sample

The 0 YBP modern travertine from AT-1 was collected as reported in Fouke et al., (2003). Field sampling of the AT-2 travertine was completed from a single sample set collected during daylight on 15<sup>th</sup> June 1999 by the Fouke Lab group. Sample locations were thoroughly wiped cleaned with 10% bleach to avoid contamination from the environment. Samples were then cut using scapula blades and collected with spatula.

### 3.1.3 ~100 YBP Recent NHT Travertine sample

The Fouke Lab group collected sub-recent Holocene travertine samples from NHT of the MHS in August 1999. A Shaw Tool Company backpack core drill (Shaw Tool, Yamhill, Oregon) was used to take in situ samples from NHT deposit. One of the samples from the proximal slope facies from this deposit was used in this study.

#### 3.1.4 ~4000 YBP Holocene USGS drilled Y-10 Core Travertine sample

Travertine near Bath Lake cored by USGS in 1967 (Y-10 Core) is stored at the USGS Core Research Center in Denver, CO. A number of samples from various depths of the core were taken from this core facility for analysis.

#### 3.1.5 ~30,000 YBP Late Pleistocene Gardiner Travertine sample

The Fouke Lab group collected travertine samples from Gardiner in June of 2006 over the period of 5 days from June 12 through June 17 as follows (Butler, 2007). A Shaw Tool Company backpack core drill (Shaw Tool, Yamhill, Oregon) was used to take in situ samples from clean-cut Gardiner quarry surfaces. Cores range in length from 23 cm to 36 cm with a diameter of approximately 5 cm. Samples were measured with a 10 m soft tape measure, placed in sample bags, labeled, sealed and transported back to the lab. A sample from the proximal slope facies (GQ\_PS) was analyzed in this study.

#### 3.1.6 ~1.1Ma YBP Middle Pleistocene Cakmak Travertine sample

The Ozkul Lab group (KU Leuven, Belgium) collected samples in July of 2013. The samples were taken with a STIHL MS261 drilling device (1 inch drill bit) from the vertical quarry exposure walls. Prior to each sampling spot, the drill bit outer and inner surfaces were rinsed and cleaned with autoclaved MilliQ water, 70% ethanol and 10% bleach. Samples were removed from the quarry wall with a sterile spatula, packed in a labeled, sterile falcon tube and stored in a liquid nitrogen-cooled Dewar (-80°C) for shipping. A sterile water tank filled with autoclaved MilliQ water was used for cooling during drilling. Samples were stored at -80°C upon arrival at

the University of Illinois at Urbana-Champaign. One of the samples was analyzed from the Proximal Slope environment, exposed in the Cakmak quarry (CM\_PS).

### 3.2 Preparation of Travertine Sample Powders

All sample preparations and DNA extractions were completed in an ancient DNA laboratory facility in the Institute for Genomic Biology at the University of Illinois Urbana-Champaign. A description of the facility is given below.

#### 3.2.1 Modern-Holocene sample preparation

The modern sample from AT-2 (AT2\_PS) was thoroughly wiped clean with Kimwipe soaked in 6% sodium hypochlorite (100% Clorox bleach) for at least 1 min to remove surface contaminants, rinsed with molecular grade DNA-free water and dried under UV light in a UV crosslinker. This sample broke apart easily and therefore did not require drilling. It was instead broken and ground to produce ~5.0 grams fine powder using a mortar and pestle for DNA extraction purposes.

#### 3.2.2 Sub-recent Holocene sample and Ancient Pleistocene sample preparation

The sub-recent Holocene sample (HT\_PS) and ancient Pleistocene samples (YC\_PS, GQ\_PS, and CM\_PS) were thoroughly wiped clean with Kimwipe soaked in 6% sodium hypochlorite (100% Clorox bleach) for at least 1 min to remove surface contaminants, rinsed with molecular grade DNA-free water and dried under UV light in a UV crosslinker. Approximately 5.0 grams of travertine powder was obtained from each sample for DNA extraction using a dremmel tool at low speeds to minimize the production of heat.

### 3.3 Molecular Microbiology Analyses

#### 3.3.1 Clean Room Conditions

All sample preparations, DNA extractions and PCR amplification setups were completed in the Institute for Genomic Biology Core Facilities Ancient DNA Laboratory dedicated solely to ancient DNA work. Strict protocols were followed to minimize the amount of human and bacterial DNA contamination in the ancient DNA laboratory. The ancient DNA lab is a positively pressured clean room with hepa-filtered air. The clean room contains an anteroom and air flows from the ancient DNA lab to the anteroom to the hallway. Personnel working in the ancient DNA lab wear surgical gloves, disposable hairnets, facemasks, laboratory coveralls and booties. All consumables, disposables, tools and instruments are externally bleached and cleaned using DNA off and UV irradiated before entering the lab and then subjected to routine cleaning before, during and after use. Separate working hoods are dedicated to sample preparation (cleaning, and drilling/grinding), DNA extraction and isolation as well as PCR. Finally, the ancient DNA lab is also routinely cleaned with bleached.

#### 3.3.2 DNA Extraction

DNA extraction and isolation from fossil travertine were carried out in the clean room described under little or no contamination conditions as described above. The PowerLyzer PowerSoil DNA Isolation Kit (MoBio Inc, CA) was used for the extraction of genomic DNA from the all travertine samples using a protocol slightly modified from that of the manufacturer. Briefly, bulk travertine samples were cleaned; drilled or ground to produce about 5.0 grams of powdered travertine sample as described above. The travertine powder was then incubated in 10 ml of demineralization/lysis buffer (0.5 M EDTA, 33.3 mg/ml Proteinase K and 10% N-lauryl

sarcosine) for digestion overnight (12-24 hours) at 37°C. The digested samples were then centrifuged and supernatant transferred into Amicon Ultra-15 centrifugal filter units and concentrated to about 250 µL. Following concentration, the digest was run through silica columns using the PowerLyzer PowerSoil DNA Isolation Kit (MoBio Inc, CA) and eluted in 60 µL volume of DNA extract. A negative control was prepared following the same protocol without using any powdered sample.

### 3.3.3 Polymerase Chain Reaction (PCR) Amplification

Samples were amplified using the polymerase chain reaction (PCR), with a mix as follows: 2.00 µL L genomic DNA, 12.62 µL molecular-grade water, 2.00 µL 10x PCR buffer, 1.20 µL 50 mM MgCl<sub>2</sub>, 0.80 µL 10 mM dNTPs, 0.60 mL of each 10 µM primer, and 0.18 µL HiFi Platinum Taq DNA Polymerase (Life Technologies). The PCR was performed using the following primer set for Bacteria: 8F (5'-AGA GTT TGA TCC TGG CTC AG-3') and 1492R (5'-GGT TAC CTT GTT ACG ACT T-3') (Liu et al., 1997b). PCR product was confirmed with agarose electrophoresis and quantitative DNA ladder (Hyperladder I, Bioline USA, Boston, MA). DNA samples were loaded onto 1% agarose gel, stained with ethidium bromide and visualized under UV light. Considering the precaution of contamination, appropriate negative controls were used to ensure no sample was contaminated with exogenous DNA. A negative procedural control containing no sample prepared during DNA used tested as well. No DNA was detected in the negative control extraction by gel electrophoresis, and no amplification was observed in any PCR reactions using this sample as a template. The amplified PCR products were purified with Qiaquick PCR purification kit (Qiagen Inc., CA) following the manufacturer's protocol.



### 3.3.4 Terminal-Restriction Fragment Length Polymorphism (T-RFLP)

Community profiles were generated using T-RFLP in order to determine the modern-to-ancient transact phylogenetic diversity preserved in proximal slope facies travertine samples analyzed (Liu et al., 1997). This technique is used to distinguish microbial populations within a sample by tagging a PCR-amplified gene with a fluorescent marker, then cutting the gene into fragments using a series of restriction enzymes; the size of a tagged fragment is characteristic of the population from which the gene was obtained (Liu et al., 1997). Full-length 16S rRNA genes were amplified from genomic DNA using FAM-labeled 8F (5'-AGA GTT TGA TCC TGG CTC AG-3') and 1492R (5'-GGT TAC CTT GTT ACG ACT T-3') as described above.

The purified PCR products were digested using restriction enzymes *RsaI* and *MspI* (New England Biolabs Inc., MA) in a single reaction using the CutSmart™ Buffer at 37°C for an hour. Using two separate digestion enzymes ensures that the tagged fragments from phylogenetically distinct microbial populations differ in length (Marsh, 2005). The digested samples were then analyzed with an AB 3730xl DNA Analyzer using ROX1000 (Applied Biosystems) at the Roy J. Carver Biotechnology Center at the University of Illinois at Urbana-Champaign for fragment analysis.

A peak profile table of fragment size and intensity was created from the fluorescent intensity of each terminal restriction fragment using the GeneMapper® v5.0 software (Applied Biosystems). We eliminated peaks with a size less than 50 or greater than 1000 base pairs, (the limits of the 1000 ROX size standards) for each sample. This procedure is important in preventing uncut DNA or large terminal fragments from contributing to the profile. Profiles were then visually

examined to ensure that these two types of fragments did not contribute significantly to the profile.

To ensure that only peaks representing actual populations were considered, peaks with a height of less than 50 absorbance units were eliminated. We then normalized each individual peak height to the sum of all peak heights for the sample. This step is important in standardizing the results for statistical comparison. For the statistical analyses, we assumed each terminal fragment represents a single population (Rees et al., 2004).

To further analyze and compare microbial communities of the various samples, we calculated the average number of T-RFLP peaks found in each sample. We then use a number of multivariate statistical analyses within the programming and visualization environment R v. 3.1.2 (R Development Core Team, 2014) to quantify the similarities and differences between the modern and ancient communities. The “vegdist” function was used to compute the distance (dissimilarity) between both rows and columns (<http://www.inside-r.org/packages/cran/vegan/docs/vegdist>); while the “hclust” function was employed to compute the hierarchical cluster analysis on a set of dissimilarities and methods for analyzing it (<http://www.inside-r.org/r-doc/stats/hclust>). This is an average clustering algorithm also known as Unweighted Pair Group Method with Arithmetic Mean (UPGMA). The dendrogram was constructed by means of an agglomerative clustering algorithm in order to cluster both the rows and columns of tabular data separately (<http://www.inside-r.org/r-doc/stats/is.leaf>). The metaMDS tool, which performs Nonmetric Multidimensional Scaling (NMDS), and finds the

lowest stress, was used to visualize the level of similarity of individual cases of a dataset (<http://www.inside-r.org/packages/cran/vegan/docs/initMDS>).

### 3.3.5 V3-V5 16S rRNA Hypervariable Region Sequencing

Genomic DNA was extracted from all samples as described above. The size and intensity of the genomic DNA were confirmed with agarose electrophoresis and quantitative DNA ladder (Hyperladder I, Bioline USA, Boston, MA) when they were loaded onto 1% agarose gel, stained with ethidium bromide and visualized under UV light. Bulk extractable genomic DNA concentrations were also measured using the Quant-iT™ dsDNA High-Sensitivity Assay Kit (Life Technologies Inc.). Genomic DNA samples were then sent to the Roy J. Carver Biotechnology Center at the University of Illinois at Urbana-Champaign for amplicon library synthesis on the Fluidigm Access Array™ System. The Access Array™ System is comprised of a thermal cycler, a pre-PCR IFC Controller AX for loading samples, and a post-PCR IFC Controller AX for harvesting amplified products. Output of the system results in pooled amplicons flanked by barcoded Illumina linkers ready for sequencing on the MiSeq. This system significantly reduces the time required for enrichment of targeted sequences by combining amplicon generation with library preparation. The cite specific 357F (CCTACGGGAGGCAGCAG) and 926R (CCGTCAATTCMTTTRAGT) primers modified with Fluidigm CS1 and CS2 tails respectively were used to amplify the V3-V5 region of the bacterial 16S rRNA gene.

### 3.3.6 Bioinformatics

Using the sample specific barcodes assigned during sequencing, the sequenced data was developed and demultiplexed in QIIME 1.8.0 (Table 3; Caporaso et al., 2010). Sequences were trimmed using Trimmomatic 0.32 (Bolger et al.,) and those found to be too short, removed in the process. Successful sequences were then aligned using the default QIIME pipeline of aligning reads (PyNAST) to the Greengenes Core reference alignment, and unaligned sequences removed (Caporaso et al., 2010; DeSantis et al., 2006). OTUs were picked using the “Closed” OTU picking option (pick\_closed\_reference\_otus.py), which clusters at 97% sequence similarity with uclust (Edgar 2010) by comparing the sequences to the Greengenes Core reference genes in QIIME. Representative sequences were picked for each OTU for downstream analysis since each OTU may be made up of many related sequences. Taxonomy was then assigned at 97% similarity based on the Greengenes taxonomy and a Greengenes reference database (Version 12\_10) (McDonald et al., 2012). This provides information on the microbial taxa found in the samples. The default uclust consensus taxonomy classifier was in used for the taxonomy assignment in QIIME. The sequences were aligned through assignment to an existing alignment with PyNAST also using QIIME. Before inferring a phylogenetic tree relating the sequences, the sequence alignment was filtered to remove columns comprised of only gaps, and locations known to be excessively variable. A phylogenetic tree was then produced using the filtered aligned V3-V5 sequences of the modern and ancient sequences generated for the hypervariable region using PyNAST.

Following taxonomy assignment, the sequenced data was further processed in QIIME and fundamental output of the comparisons in a square matrix where a “distance” or dissimilarity is

calculated between every pair of community sample, reflecting the dissimilarity between those samples. To remove heterogeneity, rarefaction was performed on the OTU table to standardize all samples and to compare OTU richness on a standardized platform. The weighted version of the UniFrac metric, which accounts for the relative abundance of each of the taxa within the communities, was used in this analysis. Weighted Unifrac distances calculated were visualized using the Principal Co-ordinates Analysis (PCoA) using EMPERor, an interactive next generation tool for the analysis, visualization and understanding of high throughput microbial ecology datasets (Vázquez-Baeza et al., 2013). The workflow further uses jackknife to estimate the uncertainty in PCoA plots and hierarchical clustering of microbial communities, which can be visualized using FigTree (FigTree v1.4.2).

## CHAPTER 4:

### RESULTS

#### 4.1 Genomic DNA extraction and PCR amplification

Microbial DNA from all five modern-to-ancient proximal slope facies travertine samples was successfully extracted and PCR amplified. Very low amounts of genomic DNA ( $\sim 0.1 \text{ ng}/\mu\text{L}$  –  $5 \text{ ng}/\mu\text{L}$ ) were however recovered from  $\sim 5.0 \text{ g}$  of powdered travertine samples. Bulk extractable genomic DNA concentrations measured using the Quant-iT™ dsDNA High-Sensitivity Assay Kit (Life Technologies Inc.) showed general decrease with increasing age and diagenetic alteration of travertine samples (Table 3 and Fig. 6).

#### 4.2 Changes in Microbial Phylogenetic Diversity in Modern-to-Ancient Proximal Slope Facies Travertine

##### 4.2.1 T-RFLP Profiles

Direct comparison of the T-RFLP profiles representing microbial communities for each sample showed that a number of shared terminal restriction fragments (T-RFs) were present in all communities, but each contained unique T-RFs as well (Fig. 7). Figure 7 shows results from all five samples analyzed (9 YBP Modern Travertine sample AT2\_PS,  $\sim 100$  YBP Recent Travertine sample HT\_PS,  $\sim 4000$  YBP Holocene Travertine sample YC\_PS,  $\sim 30,000$  YBP Late Pleistocene Travertine sample GQ\_PS and the  $\sim 1.1$  Ma YBP Middle Pleistocene Travertine sample CM\_PS). Each peak (T-RFs) represents a unique microbial population. Community richness appeared to vary from one community to the other. Samples AT2\_PS and YC\_PS both have 9 terminal fragments of which 5 are shared. The same terminal fragments (12) are observed in both Recent sample HT\_PS and ancient sample GQ\_PS. Ancient sample CM\_PS appeared to have the

highest diversity with 23 terminal fragments. T-RFLP profile however may only show the major populations present in a community and not necessarily reflect the complete species richness of a given sample. Results from the hierarchical cluster analysis showed two broad divisions. Samples AT2\_PS and YC\_PS formed one branch while samples CM\_PS, HT\_PS and GQ\_PS formed the second branch. This is representative of the species richness observed in the samples. Visual clustering from MDS showed similar distribution observed from the hierarchical clustering.

#### 4.2.2 16S rRNA Sequenced library diversity

The 16S rRNA gene sequences were further analyzed by high throughput sequencing on the Illumina Miseq sequencer targeting the V3-V5 hyper-variable region of 16S rRNA genes. It is worth mentioning that the sub-recent Holocene sample HT\_PS, from the New Highland Terrace (MHS) produced only 17 sequences during Miseq sequencing. Further analysis was impossible as no meaningful sequences were obtained after demultiplexing and quality filtering (Table 4). No OTUs were therefore obtained from this sample for further analysis. Table 4 shows a summary of the resulting number of 16S rRNA gene sequences before and after quality filtering. As follows: 86698 from the sample AT2\_PS, 47609 from the sample YC\_PS, 34970 from sample GQ\_PS and 48903 from the sample CM\_PS. This resulted in the recovery of over 400 OTUs with sequences related to 15 bacterial phyla and ~95 species from all samples analyzed (Table 4 and Fig. 6).

Relatively higher diversity assemblage of bacterial sequences was detected in the sample AT2\_PS in comparison to diversities observed in samples YC\_PS, GQ\_PS and CM\_PS (Tables

6, 7, 8 and 9 respectively). This is in contrast to the highest species diversity observed from the T-RFLP profiles. Microorganism identifications were based on comparison of these sequences with the GenBank database using the BLAST tool. Phylum-level microbial diversity in each sample was estimated by dividing the number of sequences representing each phylum by the total number of sequences in each sample (Fig. 8).

#### 4.2.2.1 Microbial communities inhabiting 0 YBP Modern Travertine sample (Fouke et al., 2003)

Fouke et al., (2003) constructed clone libraries and sequenced the selected unique clones for sequence analysis using patterns from T-RFLP analysis conducted. Results showed that sample AT1\_PS was dominated mainly by sequences related to Proteobacteria (~38%), which also had the highest diversity (13 orders). Significant contributions were from sequences related to following orders: Rhodospirillales, Enterobacteriales, Hydrogenophilales, Burkholderiales, Caulobaterales and Xanthomonadales.

This is followed by sequences related to Cyanobacteria (~18%), with significant contributions from Sequences related to Pseudanabaenales, Synechococcales, Gloebacterales and Oscillatoriales. Phyla Aquificae (15%), Chlorobi (~11%), Bacteroidetes (7%), and Chloroflexi (~5%) also made significant contributions to the microbial composition of this sample. With total of ~40 families from 11 phyla represented, sample AT1\_PS had the second highest microbial diversity (Fig. 9A). Having lower diversity than AT2\_PS could be explained by the different method of analysis employed for this sample.



#### 4.2.2.2 Microbial communities inhabiting 9 YBP Modern Travertine sample

The modern Holocene sample AT2\_PS, appears to be dominated mainly by sequences related to Cyanobacteria (~47%). These are made up mainly of related sequences in the orders of Pseudanabaenales, Synechococcales, Gloebacterales and Oscillatoriales.

This is followed by sequences related to Proteobacteria (~25%), which presented the highest diversity (13 orders) with significant contributions from Rhodospirillales, Enterobacteriales, Myxococcales, Burkholderiales, Sphingomonadales and Xanthomonadales. Sequences related to Chloroflexi (~13%) and Chlorobi (~14%) also made significant contributions to the microbial composition of this sample. With total of ~47 families from 11 phyla represented, sample AT2\_PS had the highest microbial diversity (Fig. 9B).

#### 4.2.2.3 Microbial communities inhabiting ~4,000 YBP Holocene Travertine from Y-10 Core

The 16S rRNA gene sequences indicated that ancient Holocene sample YC\_PS contained relatively different assemblage of bacterial sequences in comparison to the modern sample AT2\_PS. The microbial community composition was dominated mainly by sequences related to three orders (Bacillales, Lactobacillales and Clostridiales) belonging to the phylum Firmicutes (~57%). The next most abundant sequences were related to Proteobacteria (~17%). A maximum of only ~8% of the sequences were representative of Cyanobacteria in contrast to the dominance of Cyanobacteria sequences in the modern sample. Other represented phyla include sequences related Actinobacteria (~4%), Aquificae (~4%), Thermi (~4%) and others. A total of ~19 families representative of 9 bacterial phyla were present in this sample (Fig. 9C).

#### 4.2.2.4 Microbial communities inhabiting ~30,000 YBP Late Pleistocene Gardiner Travertine

Approximately 37.5% of sample GQ\_PS was comprised of sequences related to one order (JG30-KF-CM45) representative of the phylum Chloroflexi. This is followed by relatively high number of sequences related to three orders (Bacillales, Lactobacillales and Clostridales) representative of the phylum Firmicutes (~28%) as observed in the other ancient samples. Approximately 8% of the sequences were related to Cyanobacteria as observed in the ancient sample YC\_PS in contrast to that observed in the modern sample AT2\_PS. Sequences related to other microbial phyla including Proteobacteria (~15%), Aquificae (~6%), Actinobacteria (~2%) and Thermi (~2%). This result indicates that the microbial community of GQ\_PS is different from the two communities above. With a total of 17 bacterial families from 8 phyla ancient sample GQ\_PS appears to have the lowest microbial diversity among all 4 samples analyzed in this study (Fig. 9D).

#### 4.2.2.5 Microbial communities inhabiting ~1.1 Ma YBP Middle Pleistocene Cakmak Travertine

Sequences recovered from ancient sample CM\_PS contained a high diversity of sequences, representing 22 families from 9 microbial phyla observed in all samples (Fig. 9E). This microbial composition was dominated by sequences related to three orders (Bacillales, Lactobacillales and Clostridales) from the phylum Firmicutes (~45%). This is followed by relatively high contributions from sequences related to Proteobacteria (~27%). Other significant contributions include sequences related to the bacteria phyla Cyanobacteria (~7%), Aquificae (~7%), Actinobacteria (5%), Chlorobi (~3%) and others.

#### 4.2.2.6 Results from beta diversity analysis

Both hierarchical and PCoA plots showed similar trends of clustering. The analyses reveal segregation between the modern and ancient samples. The first principle coordinate (PC1) appears to be driven by differences in age where the modern sample AT2\_PS is far removed from the ancient samples. The second principle coordinate (PC2) shows clustering possibly due to the varying number of species observed in the different ancient samples. Ancient samples YC\_PS and CM\_PS which have approximately the same number bacterial families (26) represented cluster together to the exclusion of ancient sample GQ\_PS with ~22 families represented (Fig. 11 and Fig. 13).

## CHAPTER 5:

### DISCUSSION

Based on the molecular analyses completed in this current study of modern-Holocene to ancient Middle Pleistocene PSF travertine, the details on the type, diversity, and the abundance of organisms capable of inhabiting this travertine precipitating hot spring environment have been determined. The current reconstruction of the biodiversity of the modern and ancient travertine microbial communities will play a critical role in comparing the current and future compositions of the hot spring microbial ecosystem in future studies. Results indicate that samples of different ages have completely different microbial community compositions. This is most evident by the shift in the microbial community structure from being Proteobacteria-dominated in the active travertine system to Cyanobacteria-dominated in the modern travertine sample and then to being Firmicutes-dominated in the Pleistocene-aged travertine. The following discussion evaluates the implications of these observed differences with respect to the evaluation of DNA as a biomarker in carbonates (travertine), travertine depositional facies, and microbial ecology.

#### 5.1 Evaluation of DNA as a biomarker in carbonates

Contamination by modern microbes is a major concern with studies involving geologically old samples (Willerslev et al., 2004b; Hebsgaard et al., 2005). Due to the fact that bacteria isolated from ancient samples show very high and close resemblance to modern bacteria at both morphological and molecular levels has lead to many critics questioning the real age of these isolates. Possible contaminants may be introduced naturally after the formation of the surrounding material (Hazen and Roeder 2001; Willerslev et al., 2004b; and Hebsgaard et al., 2005).

In the case of this study, the main concern is the effect of diagenetic alteration of the ancient samples after deposition. Previous studies of the Gardiner quarry samples of the YNP (Butler, 2007; Fouke, 2011) observed varying degrees of diagenetic alteration of the ancient travertine deposits. The water-rock-interaction leading to diagenesis in the porous travertine deposits is capable of introducing new microbial populations as well as removing the original populations. Petrographic analyses on the samples are therefore underway to determine to level of diagenetic alteration they have undergone in order to elucidate possible amount of contaminants introduced as a result. Microbial communities observed from the ancient samples could therefore range from entirely pristine ancient communities to entirely altered communities as two end members. It is highly plausible to speculate that, the microbial community might one be that lies somewhere between these two end member cases resulting in a community composed of both modern and ancient microbial populations.

It is also possible to introduce contaminants such as modern DNA during the collection, handling and analyses of samples (Vreeland and Rosenzweig, 2002). To address the possibility, all necessary precautions required to work on ancient samples were taken as outlined under the materials and methods section. The results obtained from phylogenetic and T-RFLP analyses of the ancient samples are therefore to a high confidence level, representative of the microbial populations present in these samples and not as a result of contamination from other samples, both modern and ancient.

Fouke et al., (2000), reported very rapid travertine precipitation rates (>2 mm/day) occur in the modern springs (Angel Terrace) of MHS. It is hypothesized that this should result in the

entombment and preservation of microbes in fluid inclusions during precipitation before degradation takes place (Fouke, 2011). These inclusions may be either intra-crystalline or inter-crystalline. Work done on 100-year-old travertine crystals from the pond faces of the New Highland Terrace showed the presence of organic matter in fluid inclusions (Fouke, 2011). Samples are currently undergoing petrographic analyses to determine the mechanisms of preservation.

## 5.2 Proximal Slope Depositional Facies (PSF)

Fouke et al., (2000) described a facies model for active MHS travertine depositional environment that includes the: (1) Vent facies; (2) Apron and Channel facies; (3) Pond facies; (4) Proximal Slope facies; and (5) Distal Slope facies. This model is based on the crystalline architecture, mineralogy and depositional morphology of the travertine, and secondarily on the geochemical and hydrological conditions of the spring water. A phylogenetic survey within the travertine facies model by Fouke et al (2003) was the first of its kind to understand the microbe-water-travertine crystal interactions that take place within each facies. Results showed strong 90% partitioning of dominant microbial Operational Taxonomic Units (OTUs) in the five-travertine depositional facies established at MHS by Fouke et al. (2003). Lipid profiles constructed using lipid biomarkers and carbon isotopes from AT-1 microbial mats by Zhang et al., (2004) also clearly reflect the changing microbial communities from the vent to the pond and the proximal slope and to the distal slope.

All samples for this study were obtained from the PSF of travertine deposits of YNP (USA) and Denizli Basin of Turkey. With a broad temperature range of 35-65°C and pH range of 6.9-8.0,

the PSF microbial community possibly comprises a mixture of moderately thermophilic, population (e.g. Cyanobacteria, Chloroflexi, Chlorobi, Firmicutes and Proteobacteria), and thermophilic population (e.g. Deinococcus-Thermus). This indicates a significantly more diverse microbial community in comparison to the vent, apron and channel and distal slope facies. This also is in agreement with the results obtained by Fouke et al., (2003) when they observed a general decreased in microbial diversity from the pond to proximal slope to the apron and channel to distal slope to the vent facies.

### 5.3 Microbial ecology

The ability of microbes to survive within each facies depends on the physical and chemical conditions (temperature, pH, light, flow rate and nutrient availability) of the flowing hot-spring water (Brock et al., 2001; Fouke et al., 2003; Bonheyo et al., 2005 and Fouke, 2011). This feedback interaction between microbes and minerals provides a means to track the ability of microbes to control travertine precipitation of carbonate crystals and their entombed microbial communities for direct application to ancient travertine deposits (Fouke et al., 2003; Kandianis et al., 2008; Fouke 2011). To the best of our knowledge, this study represents the first comprehensive characterization of the bacteria microbial communities in modern-to-ancient travertine using culture-independent methods.

Measured bulk extractable genomic DNA concentrations appeared to have declined with increasing depositional age of samples (Table 3 and Fig. 5). This is expected as the amount and integrity of DNA is known to decrease with increasing sample age due to accumulation of damage over time due to factors such as spontaneous hydrolysis and oxidation (Paabo, 1989;

Willerslev and Cooper, 2005). This results from the inability of inactive (dead or dormant) DNA molecules to be rapidly and efficiently repaired as observed in metabolically active tissues (Paabo 1989; Lindahl, 1993). Both modern samples AT1-PS and AT2-PS showed a higher diversity of OTUs defined by 16S rRNA gene sequences than the ancient Pleistocene samples. This was also reflected in the greater number of bacterial phyla observed in the modern samples (11) in comparison to the ancient samples (8 – 10). The richness estimates for the ancient samples varied from 43 – 50 OTUs (Fig. 6 and Table 4), which are similar to reported richness estimates for ancient samples (Aislabie et al., 2006, (29 – 85 OTUs); Smith et al., 2006, (49 – 57 OTUs)).

The T-RFLP profiling and 16S rRNA gene sequence libraries showed differences in microbial community composition and diversity with increasing depositional age of samples with associated increases in diagenetic alteration. Highest species richness was observed in the ancient sample CM\_PS in contrast to the highest species richness observed in AT2\_PS from 16S rRNA gene sequencing. This is not surprising as T-RFLP analysis usually reflects only the major populations in the community (Blackwood et al., 2007; Dunbar et al., 2000). Results from the 16S rRNA gene sequences show major contributions from relatively few number of bacterial phyla and minor contributions from the remaining phyla in the modern sample AT2\_PS. This was not the case in the ancient samples (YC\_PS, GQ\_PS and CM\_PS). This might explain why relatively lower number terminal fragments were detected in the modern sample, AT2\_PS in comparison to the ancient samples. Further analysis using beta diversity measures of the 16S rRNA gene sequences revealed the highest diversity in the modern sample AT\_PS and lowest in the ancient sample YC\_PS. Hierarchical cluster analysis of results showed the modern sample



AT2\_PS on top of the hierarchy with the highest diversity in comparison to the modern samples. This is not unexpected as the modern sample is from an active rapidly precipitating hot spring containing abundant microbial mats (Fouke et al., 2003 and Fouke 2011). This implies travertine precipitation is rapid enough to permit the successful entombment and preservation of microbial communities within fluid inclusions trapped during precipitation and deposition (Fouke et al., 2000; Butler, 2007 (*unpublished*) and Fouke 2011). Work done by Butler (2007) showed that the Gardiner travertine samples experienced partial but not complete diagenetic alteration as a result of water-rock-interactions when the regional end Pleistocene Pinedale glacier melted and retreated. This provided a large volume of meteoric water under saturated with respect to calcite and aragonite, which resulted in the precipitation of late stage blocky calcite crystals. These factors and others such as low water activity, low rates of nutrient exchange may have acted to limit bacterial diversity and species composition in the ancient travertine samples compared with the modern sample. Microbial communities reconstructed from these ancient samples may therefore be either highly pristine ancient, mixture of ancient and modern or entirely modern depending on the extent of diagenetic contamination and alteration of the samples. Studies are currently underway investigating the diagenetic history of the samples as well as localization of DNA in the travertine samples.

Microbial community differences between the different samples were further tested by partial 16S rRNA gene sequences in this study. Sample AT1\_PS (Fouke et al., 2003) was further tested by clone library construction and 16S rRNA gene sequencing of the unique clones identified using the T-RFLP patterns. The similarity and excellent depositional fabric preservation of the ancient proximal slope travertine deposits, when directly compared to the modern travertine

proximal slope depositional facies, imply that the initial microbial community structure was also similar in both the modern and ancient deposits (Butler, 2007; Fouke et al., 2000, Fouke 2011). This however does not appear to be the case in these modern-to-ancient samples as both T-RFLP and partial 16S rRNA gene sequencing methods suggested that the microbial communities in the modern sample and ancient samples were significantly different. This is evident in the visual clustering depicted in PCoA and hierarchical clustering plots (Fig. 11 and Fig 13). Samples appear to have clustered according to age. Increasing depositional age of samples results in increasing diagenetic alterations that would have caused changes in microbial community structure and composition (Butler, 2007; Fouke 2011). Species richness as seen from the number of OTUs and species present in the various samples decreased with increasing depositional age.

Fouke et al., (2003) reported a Proteobacteria-dominated microbial community in sample AT1\_PS in their study. This is a modern sample from the active hot spring system and serves as baseline for comparing samples analyzed in this study. The most notable difference between the microbial diversity is the shift in dominance from Proteobacteria (38%) in the active spring system (AT1\_PS) to Cyanobacteria (~47%) in the modern AT2\_PS sample. This shift to Cyanobacteria dominance was however absent in the ancient samples as a relatively low abundance (5 – 8%) was observed. Significant contributions in the modern sample (AT2\_PS) were from the *Pseudanabaena sp.* (~23%) and *Synechococcus sp.* (~17%) while the *Geitlerinema sp.* was the main Cyanobacteria found in the ancient samples. Pentecost et al., (1997) reported relatively high abundance of phototrophs mainly Cyanobacteria (*Phormidium laminosum*) associated with modern Pamukkale travertine of the Denizili Basin in Turkey. A number of other previous studies from various hot springs (pH > 6 and temperature < 72 °C) and

their associated microbial mats also observed 16S rRNA gene sequences affiliated to the Cyanobacteria communities (Weller et al., 1992; Fouke et al., 2003; Zhang et al., 2004; Osburn et al., 2011; Leon et al., 2013). Several Cyanobacteria being able to metabolize dissolved sulfide a common constituent of hot springs could be one of the reasons of their abundance (Oren, 2000). The removal of CO<sub>2</sub> due to photosynthesis by Cyanobacteria has also been suggested as one of the possible mechanisms responsible for travertine precipitation (Pentecost et al., 1997; Pentecost, 2003). The contrasting relatively low abundance observed in the ancient samples might be due to the inability of cells DNA or cells to be well preserved over long-term dormancy as well as other cells (Antibus et al., 2012). The long term integrity of Cyanobacteria DNA is not very well known even though they are known to maintain viability via their resistance to desiccation over decade long periods (Hawes et al., 1992; McKnight et al., 2007). Relatively low Cyanobacteria abundances have also been observed in other ancient samples such as the stromatolites of Hamelin pool in Shark Bay, Western Australia (Papineau et al., 2005) and the Antarctic permafrost (Gilichinsky et al., 2007).

Another shift worth noting is the relatively low amount (<1%) of sequences affiliated to the Aquificae phylum observed in the modern sample AT2\_PS. This is in contrast to the relatively high amount (~15%) observed in the active spring sample AT1\_PS and the ancient samples (~5 – 7%). Bacteria in the order of Aquificales have been isolated from a number of locations including the Octopus Spring, YNP (Jahnke et al., 2001), deep sea hydrothermal vents on the Mid-Atlantic Ridge (Reysenbach et al. 2000a), Calcite Springs in YNP (Reysenbach et al. 2000b) and terrestrial siliceous hot springs in Iceland (Skirnisdottir et al. 2000; 79–83 °C and pH 8.8, Takacs et al. 2002).

Sequences recovered in this study from AT1\_PS (Fouke et al., 2003) are also associated with the family Hydrogenothermaceae. Bacteria sequences belonging to the same family were also found at the Sylvan Spring and Obsidian Pool all of YNP (Meyer-Dombard et al., 2005). The best-matched organism found in NCBI using the BLAST tool was related to the genus *Sulfurihydrogenibium*. Known cultured organisms in this group have been shown to oxidize sulfur, hydrogen, arsenite, and selenite with a variety of electron acceptors (Nakagawa et al., 2005).

Another interesting find is the large amount (37.5%) of sequences related to the green non-sulfur bacteria (Chloroflexi) found in the ancient sample GQ\_PS. This was completely absent in the remaining two ancient samples (YC\_PS and CM\_PS). All sequences were related (~83% identity) to the aerobic chemoorganotroph, *Thermomicrobium roseum* isolated from YNP Octopus Spring microbial mats (Weller et al., 1992). Approximately 13% of sequences recovered from the modern sample were also related to uncultured Chloroflexi bacteria. The absence of sequences related to Chloroflexi in the other ancient samples may therefore be due to differences in location and not necessarily the age of samples.

In contrast to the relatively low abundance of Cyanobacteria related sequences in the ancient samples, relatively high numbers of Firmicutes-related sequences were observed in all ancient samples (28 – 57%) in comparison to the modern sample AT2\_PS (~0.4%). Sequences, which made significant contributions, were mainly related to *Trichococcus pasteurii* strain KoTa, *Paenibacillus favisporus*, *Bacillus* sp. *Fen\_H* and *Bacillus subtilis*. Even though Fouke et al., (2003) did not recover any sequences related to Firmicutes from sample AT1\_PS, relatively low

abundances (1 – 3%) were observed in other samples from two depositional facies (Apron and Channel and Pond) analyzed in the same study. This is therefore indicative of a generally relatively low abundance of Firmicute-related sequences in modern samples from this study area in comparison to the ancient samples. Retrieval of relatively large amounts of sequences belonging to endospore-forming Firmicutes from ancient samples was not unexpected. Firmicutes have been isolated from a variety of materials from hundreds to several thousand years of age due to the ability of their endospores to resist desiccation and survive under adverse environmental conditions (Kennedy et al., 1994; Shi et al., 1997; Steven et al., 2007; Rollo et al., 2007; Osburn et al., 2014; Antibus et al., 2012).

To further explore and understand the diversity in microbial community and composition of the various samples, the likely physiologies at the family level for each sample were identified. Based on the predominant metabolic activities of cultured representatives of the various bacterial families as identified in the Bergey's Manual of Systematic Bacteriology, The Prokaryotes 2014 and other publications (Bernardet et al., 2002; Nedashkovskaya et al., 2007a; Nakagawa, 2011), the families were classified as physiotypes. The identified physiotypes have included: (1) Oxygenic Phototroph "Ox Pho", (2) Anoxygenic Phototroph "Anox Pho", (3) Fermentation "Fer", (4) Chemoorganotrophic anaerobe "C org ana", (5) Chemoorganotrophic aerobe "C org aer", (6) Chemoorganotrophic mixed "C org m", (7) Chemolithoautotroph "C lit aut", (8) Pathogenic "Patho", (9) Mixed "Mixed" and (10) Unclassified "Unc". The "Mixed" physiotype included all families, which were too metabolically diverse to categorize and the "Unc" physiotype was used to describe the metabolisms for unclassified groups, Candidate Phyla and OTUs with only coarse phylogenetic affiliation.

The distribution of physiotypes within the different samples as shown in Figure 14 clearly indicates variability in the metabolic potentials of the various samples, which appears to be driven mainly by depositional age of the samples and not by location. This is not surprising given the effect of diagenetic alteration on the samples with increasing depositional age. As observed by the phylum level diversity within the samples, there were major shifts in microbial community composition from active to modern to ancient samples. There are distinct differences in the metabolic potential in active versus modern samples as well as between modern and ancient samples.

The active sample, AT1\_PS (Fouke et al., 2003) appears to be dominated by chemolithotrophic (~38%) metabolic potentials (mainly H<sub>2</sub> and S oxidations) from the *Hydrogenophilaceae* and *Hydrogenothermaceae* families. This was followed by phototrophic (~31%) metabolic potentials with contributions from a number of families including *Chlorobiaceae*, *Gloeobacteraceae*, *Phormidaceae* and *Pseudanabaenaceae*. This result is consistent with metabolism types observed in active hot spring environments with microbial mats composed of Cyanobacteria, anoxygenic phototrophic bacteria and chemolithotrophic bacteria (Meyer-Dombard et al., 2005; Nakagawa et al., 2005; Osburn et al., 2011).

The modern sample AT2\_PS, unlike the active sample AT1\_PS, had relatively low chemolithotrophic metabolic potential. It was dominated by sequences related to organisms with phototrophic (~72%) metabolic potential. This phototrophic metabolic potential was expected since sample AT2\_PS was dominated by Cyanobacteria related sequences, which are all

photosynthetic. The families, which made significant contributions, include *Chlorobiaceae*, *Rhodospirillaceae*, *Synechococcaceae*, and *Pseudanabaenaceae*.

A major shift is observed in the metabolic potential moving from the modern to the ancient samples. All three ancient samples (YC\_PS, GQ\_PS and CM\_PS) irrespective of location appear to be dominated by chemoorganotrophic (~75 – 78%) metabolic potentials. Samples YC\_PS and CM\_PS were dominated by anaerobic chemoorganotrophs while sample GQ\_PS was dominated by aerobic chemoorganotrophs. Contributions were from various families including *Thermomicrobiaceae*, *Bacillaceae*, *Moraxellaceae*, *Carnobacteriaceae*, *Anaerolineaceae*, *Enterobacteriaceae* and *Nannocystaceae*.

The variations observed in the samples may be due to differences in geographical locations as well as unknown geochemical factors contributing to temporal community dynamics. Possible increases in the diagenetic alteration of samples with age may also be responsible for the shifts in microbial populations observed over time. Further microbial community and geochemical comparisons of these travertine deposits are needed to better understand the factors driving the microbial community compositions observed. Samples should be analyzed from the remaining travertine depositional facies in order to elucidate differences due to changes in facies in a time series transect.

## **CHAPTER 6:**

### **CONCLUSIONS**

In this study we present the results of a systematic evaluation of the mechanisms and products of microbial community preservation within modern-to-ancient travertine from the proximal slope depositional facies. Modern travertine samples from the MHS of the YNP were directly compared with analogous Holocene-Late Pleistocene PSF travertine at Gardiner, Montana, and Middle Pleistocene PSF travertine in Denizli, Turkey.

Genomic DNA recovered from all samples showed significant decreases in concentration with increasing travertine depositional age of samples. Species richness estimates as observed from the number of OTUs were within the ranges reported by previous studies and also decreased with increasing travertine depositional age of samples.

Results from T-RFLP profiles showed the highest microbial community diversity in the ancient sample CM\_PS, while the highest microbial community diversity in 16S rRNA gene sequence libraries was observed in the modern sample AT2\_PS. This difference could be explained by biases created by the different methods. T-RFLP is known to mainly reflect the major populations in the community and therefore could result in biases against under represented populations.

Observed microbial community diversities at the phylum level consistently exhibited a shift from a Proteobacteria-dominated active spring samples to a Cyanobacteria-dominated modern travertine samples and finally to a Firmicutes-dominated ancient travertine samples. The



dramatic shift in microbial community structure between the modern and ancient travertine samples might be explained by several processes, including but not limited to the following: (1) increasing extents of water-rock interaction (diagenesis) with increasing age; (2) differential survival and persistence of the Firmicutes spore states under differing yet harsh environmental conditions.

Further analysis on the basis of physiotypes identified at the family level showed clear variability in the metabolic potentials of the samples analyzed. Results showed samples of all ages contain phototrophic, chemotrophic and heterotrophic metabolic activities. The active spring sample was dominated by chemolithoautotrophic metabolic potentials, the modern sample dominated by phototrophic metabolic potentials and all three ancient samples dominated by chemoorganotrophic metabolic potentials.

The similarity and excellent depositional fabric preservation of the ancient proximal slope travertine deposits, when directly compared to the modern travertine proximal slope depositional facies, imply that the initial microbial community structure was also similar in both the modern and ancient deposits. All changes observed must therefore be due mainly to differences in travertine depositional ages of the samples analyzed.

## CHAPTER 7:

### FIGURES AND TABLES

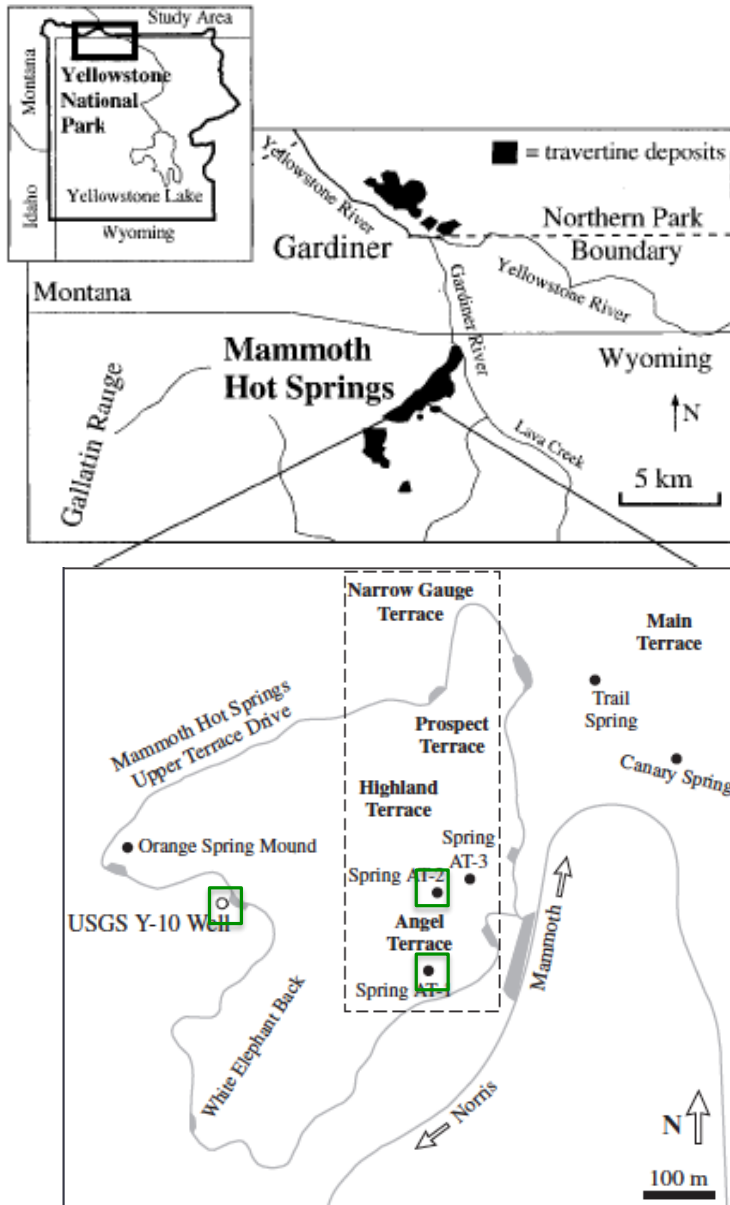


**Fig. 1:** Geographic location of Mammoth Hot Springs in Yellowstone National Park, Wyoming. Map inset shows the location of Angel Terrace Springs (AT-1, AT-2 and AT-3) within the New Highland area of Mammoth Hot Springs and the USGS Y-10 Well. (Modified from Fouke et al., 2000 and Fouke, 2011)

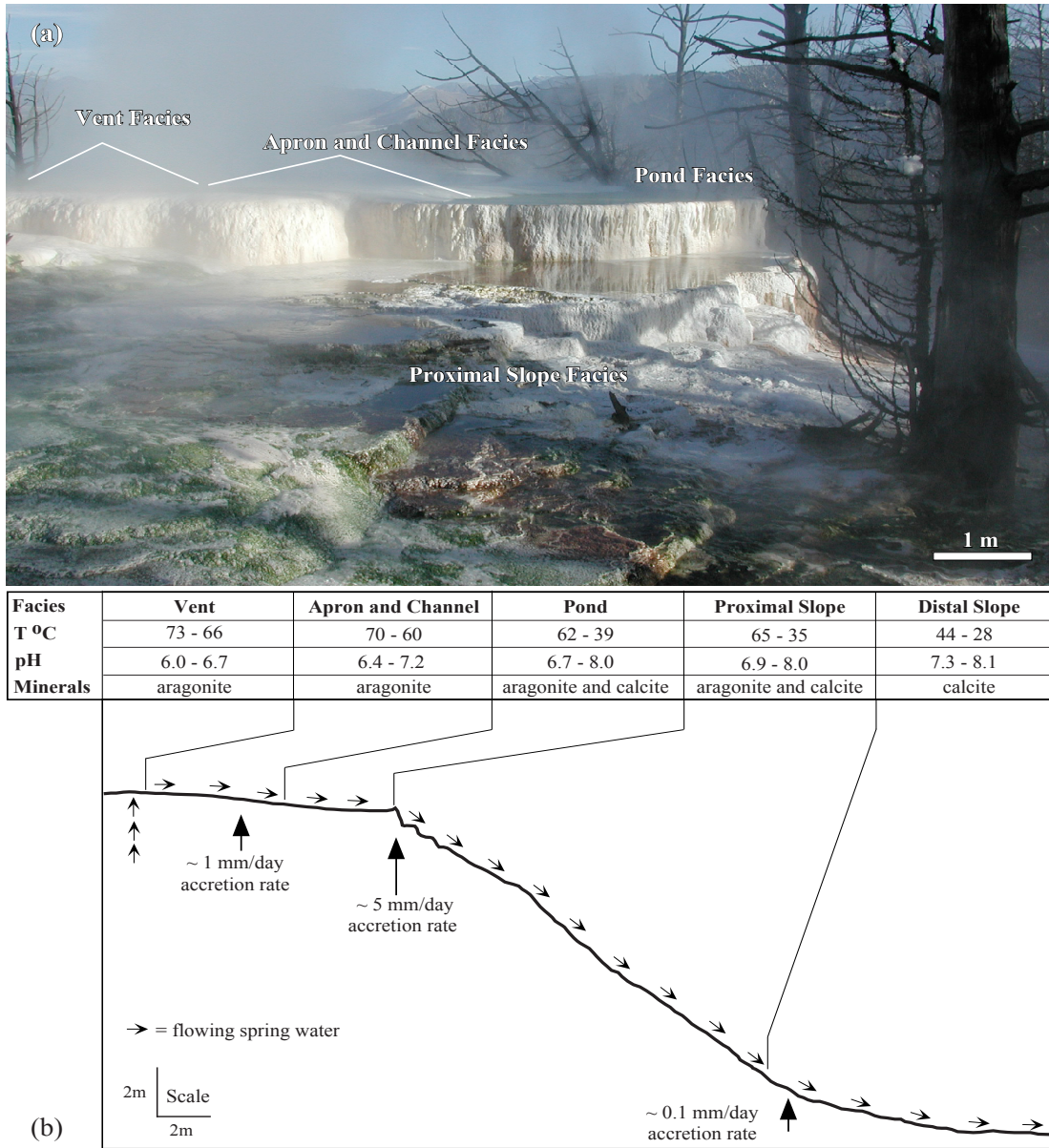


**Fig. 2:** Travertine depositional facies at Mammoth Hot Springs. (A) Field photograph of Angel Terrace Spring AT-1. (B) Schematic cross-section of the travertine depositional facies (Fouke et al., 2011).

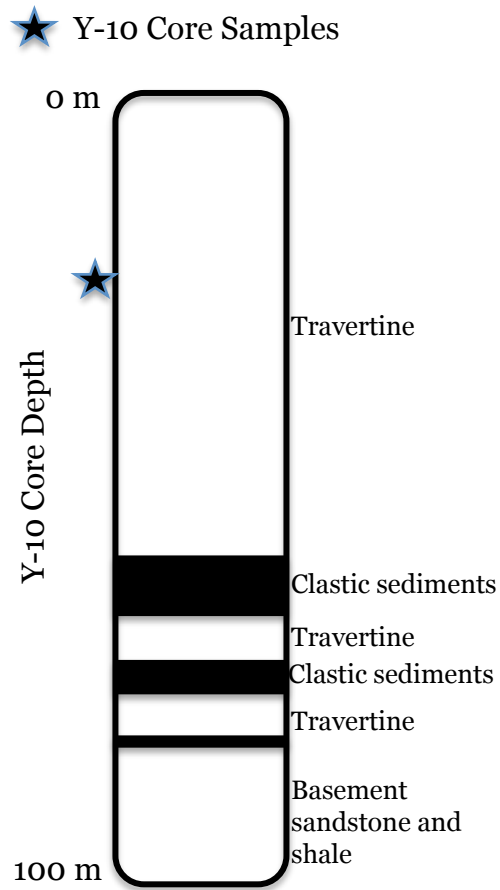


**Fig. 3:** A USGS Y-10 Core at Mammoth Hot Springs. Stars indicate depths from which samples for this study were (Modified from Sorey, 1991).

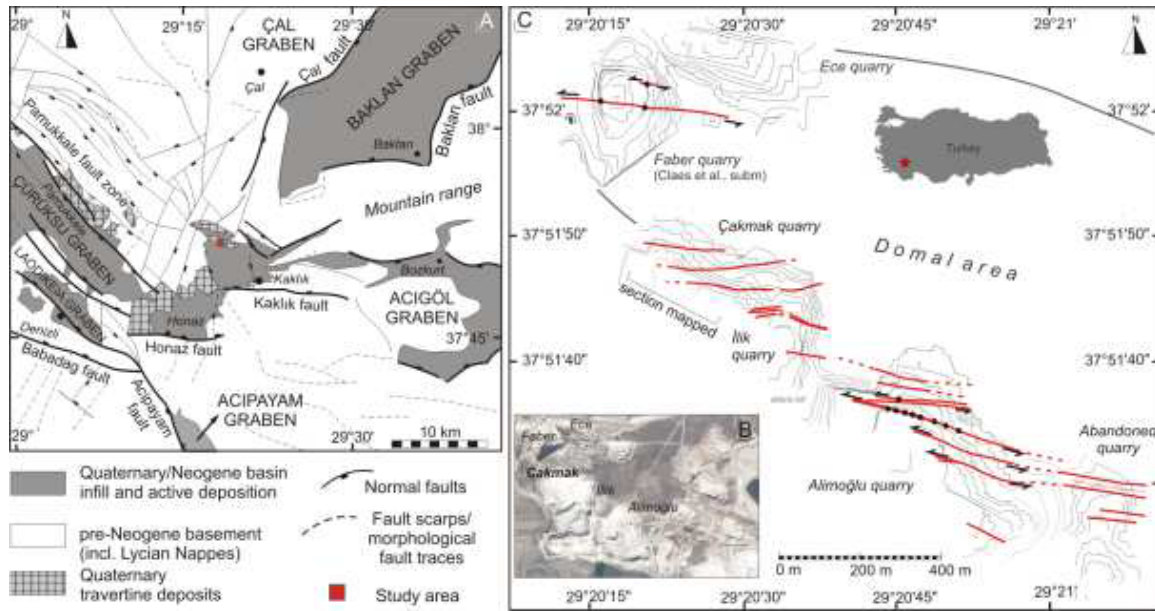


**Fig. 4:** Structural geological setting of the Cakmak quarry, Ballık area, Turkey (modified after Van Noten et al., 2013). **A.** Location in the Denizli Basin at the cross-section of the Cürüksu, Baklan en Acıg.l Grabens. **B.** Satellite view of whitish travertine exposures (now quarried) at the Ballık “domal” area. **C.** Location of the Cakmak quarry in the Ballık “domal” area. Outline of the different quarries is based on Lidar data (From De Boever et al., 2015).

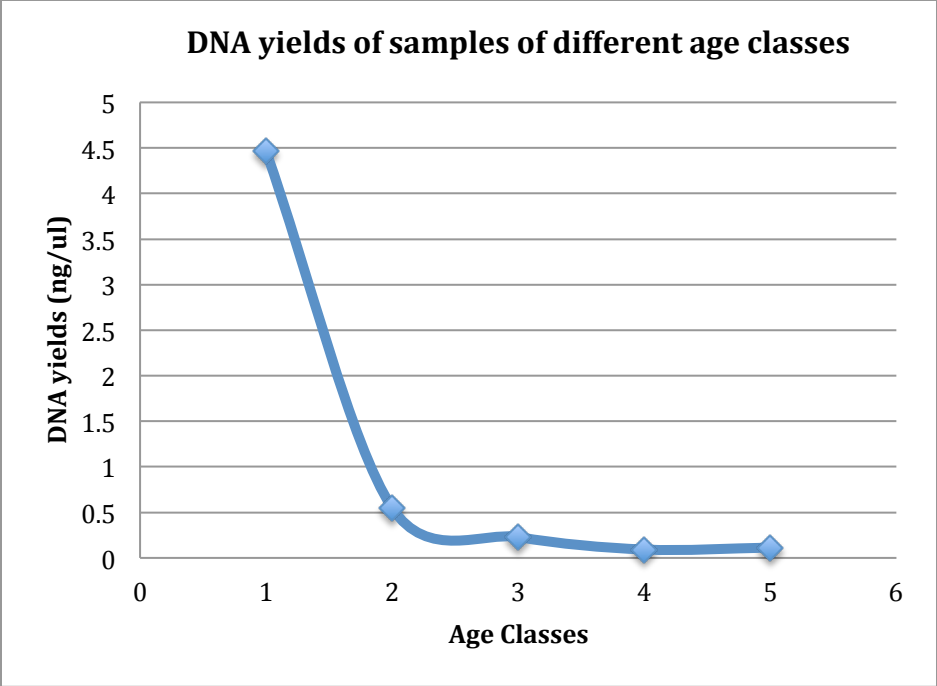


**Fig. 5:** Decreasing genomic DNA yields with increasing sample age. Ages were divided into 5 classes with 1 being the youngest samples and 5 being the oldest samples

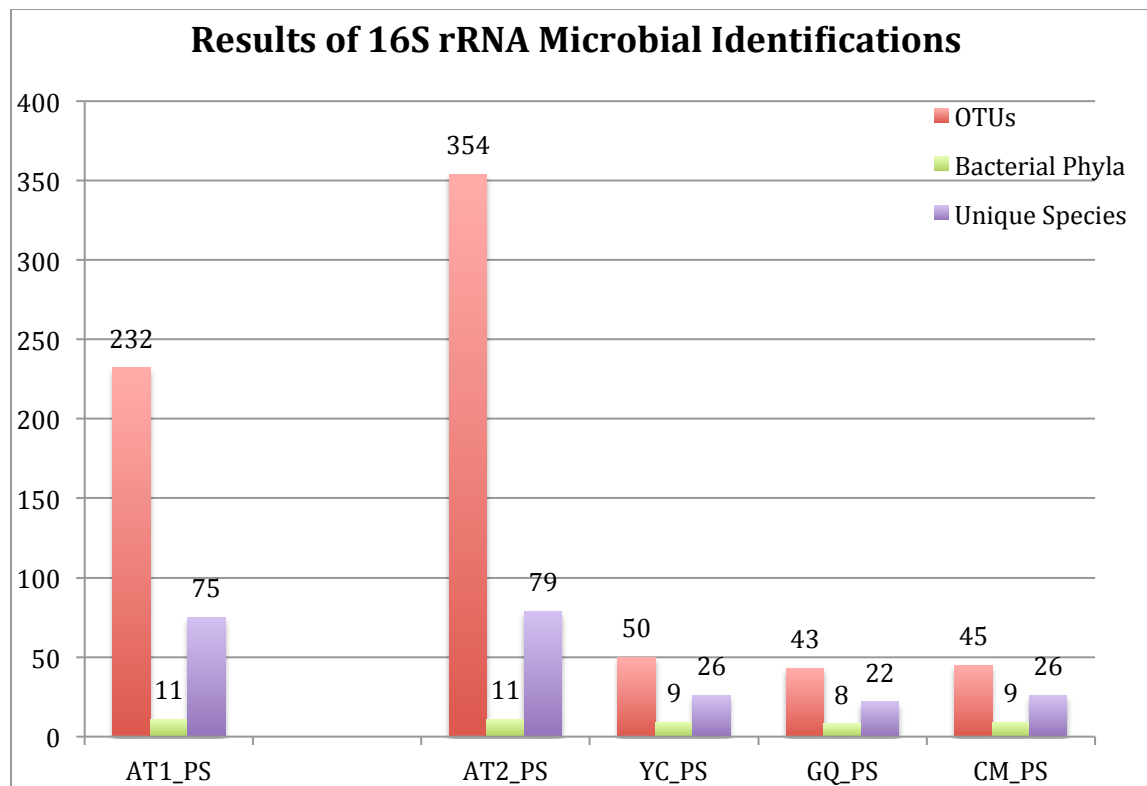


**Fig. 6:** Histogram summary of the molecular microbiology analyses completed by Fouke et al., 2003 (AT1\_PS) and in this study, including the number of OTUs, affiliated Bacterial phyla and inferred Unique Species The total.

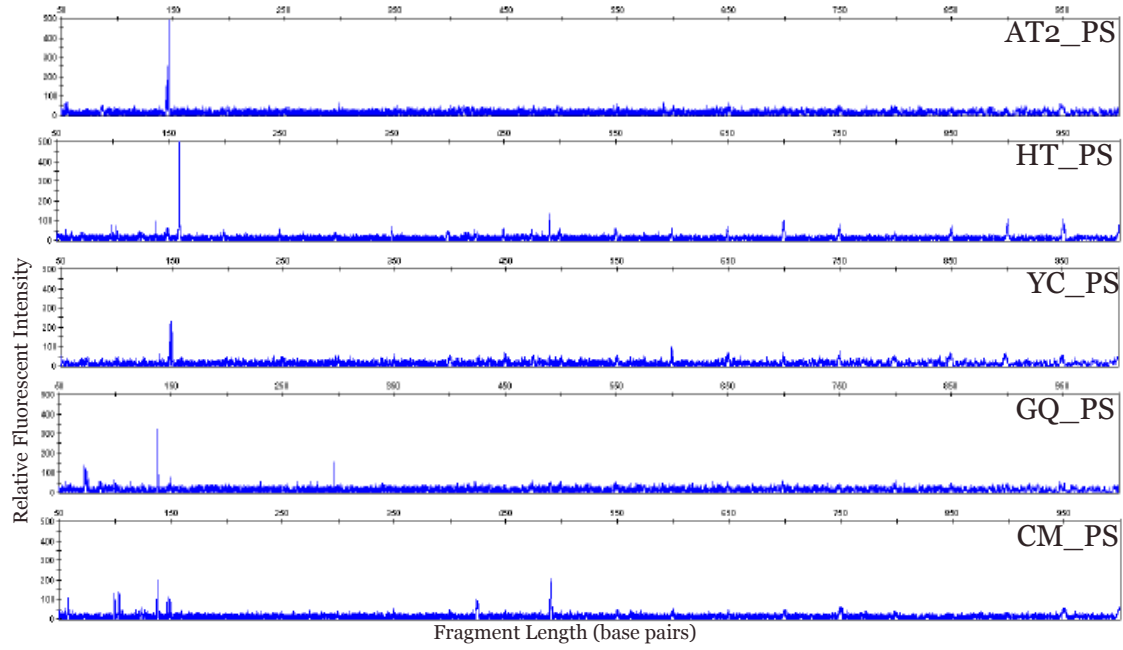


**Fig. 7:** T-RFLP profiles of the microbial communities within modern through ancient travertine samples. Samples from the PSF were compared based on the age of the travertine depositional facies



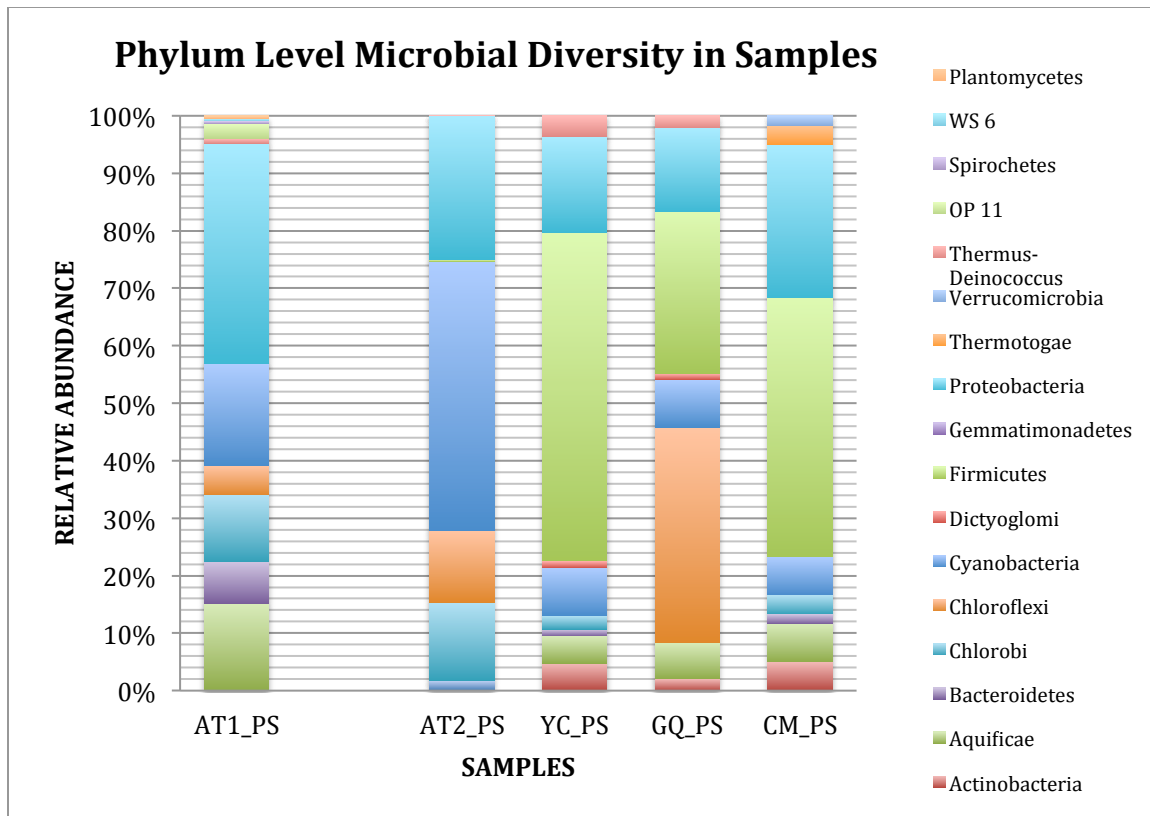


**Fig. 8:** Phylum-level microbial community composition of samples was also compared on a facies level through time. All samples are from the proximal slope facies from different locations and ages. All the ancient samples (YC\_PS, GQ\_PS and CM\_PS) have very high amounts of Firmicutes, which is low in the modern sample, AT2\_PS. Ancient sample GQ\_PS from the Gardiner relatively high amount Chloflexi which almost absent in the other ancient samples. All samples also have other shared and unique phyla

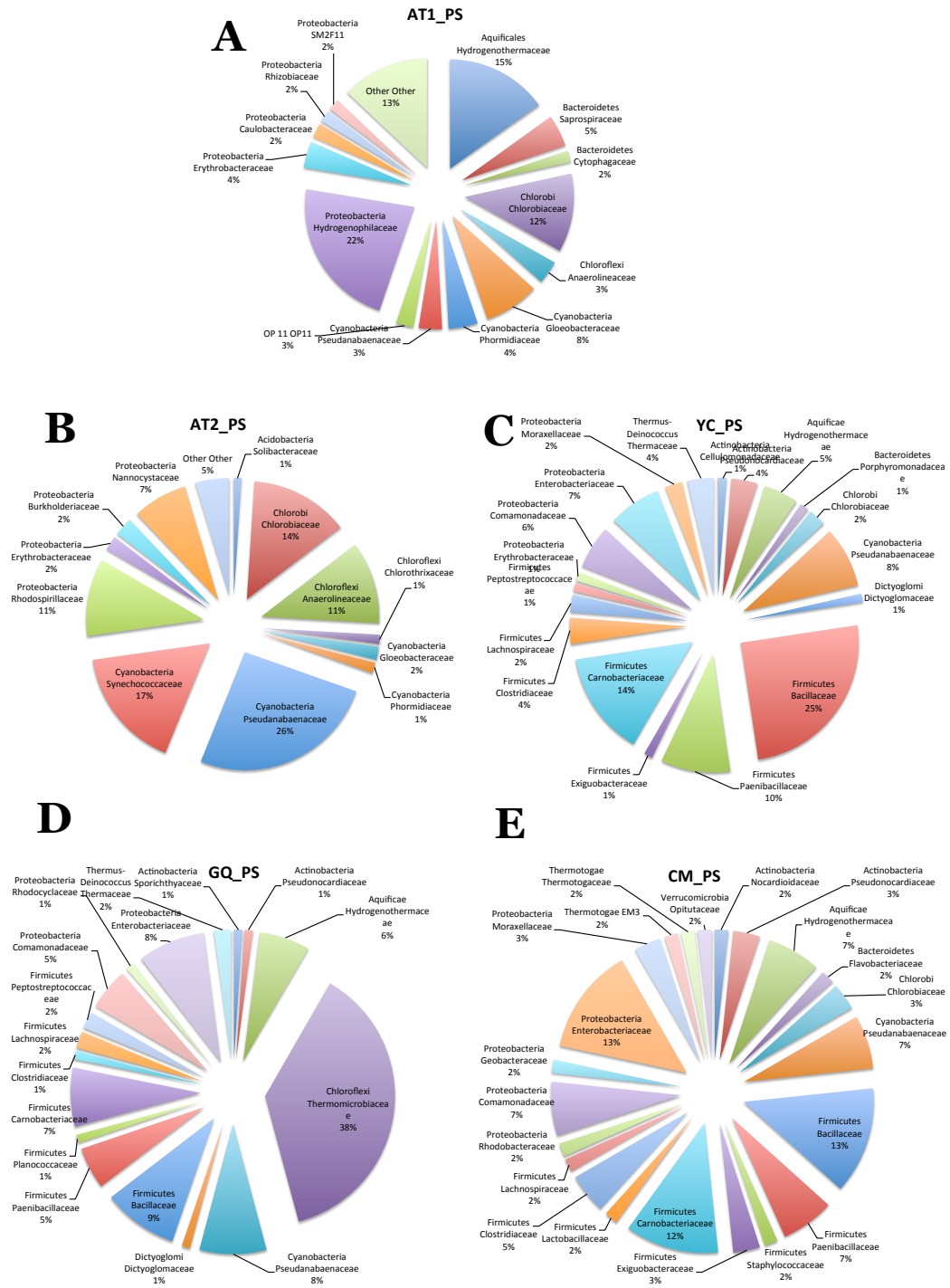


**Fig. 9:** Family-level microbial composition of individual samples from all traverdine depositional facies and ages.

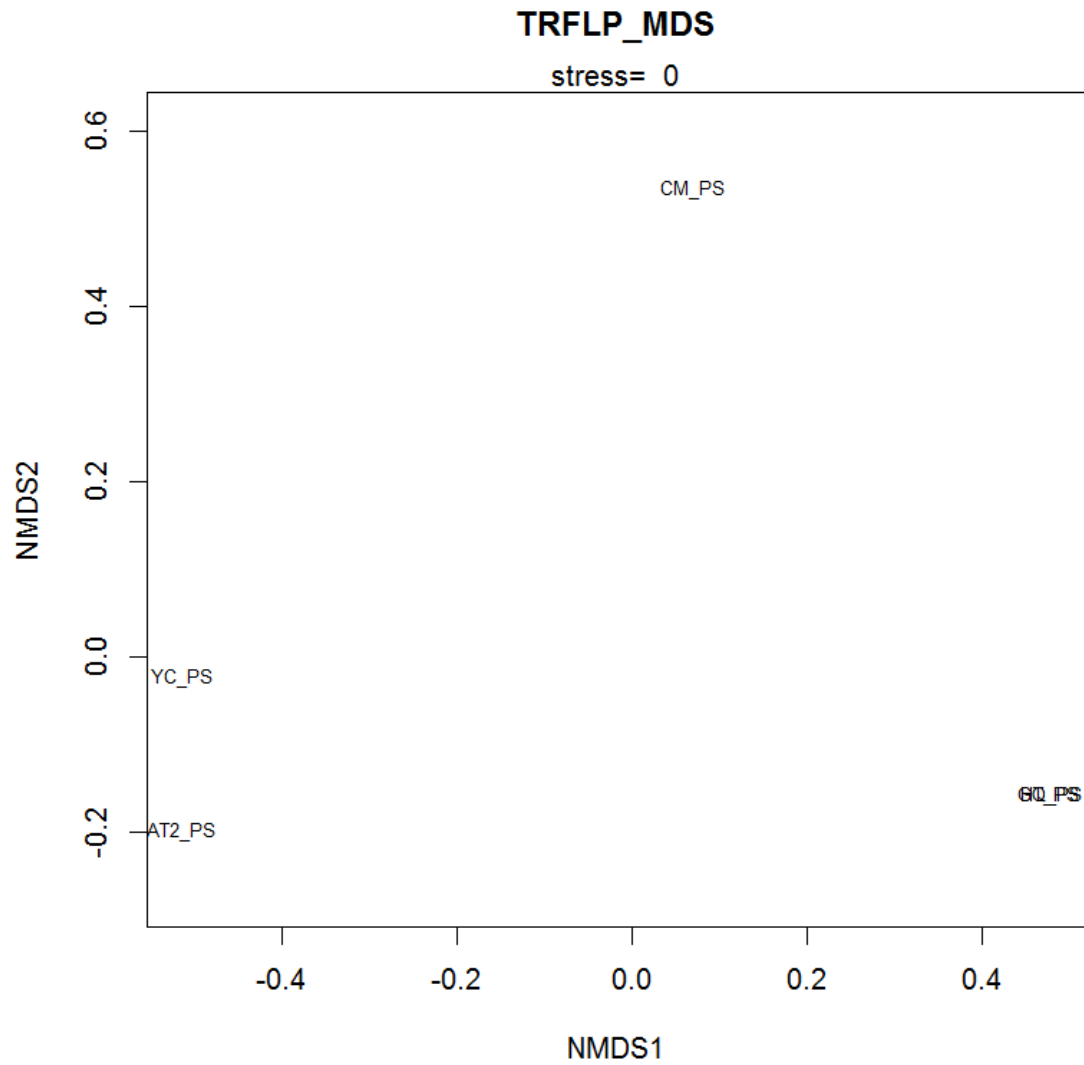


**Fig. 10:** Visual Clustering of microbial community compositions from of all samples all travertine depositional facies. Analysis was based on the data from the T-RFLP profiles generated.

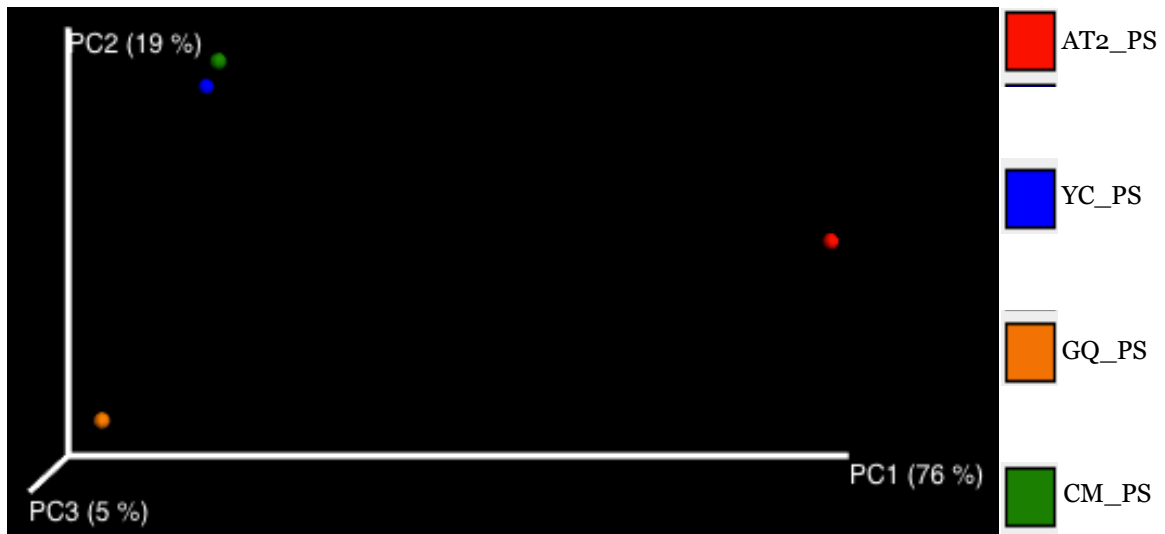


**Fig. 11:** Visual Clustering of microbial community compositions of all samples from the from all travertine depositional facies. AT2: Analysis was based on data from the 16S rRNA gene sequence libraries.

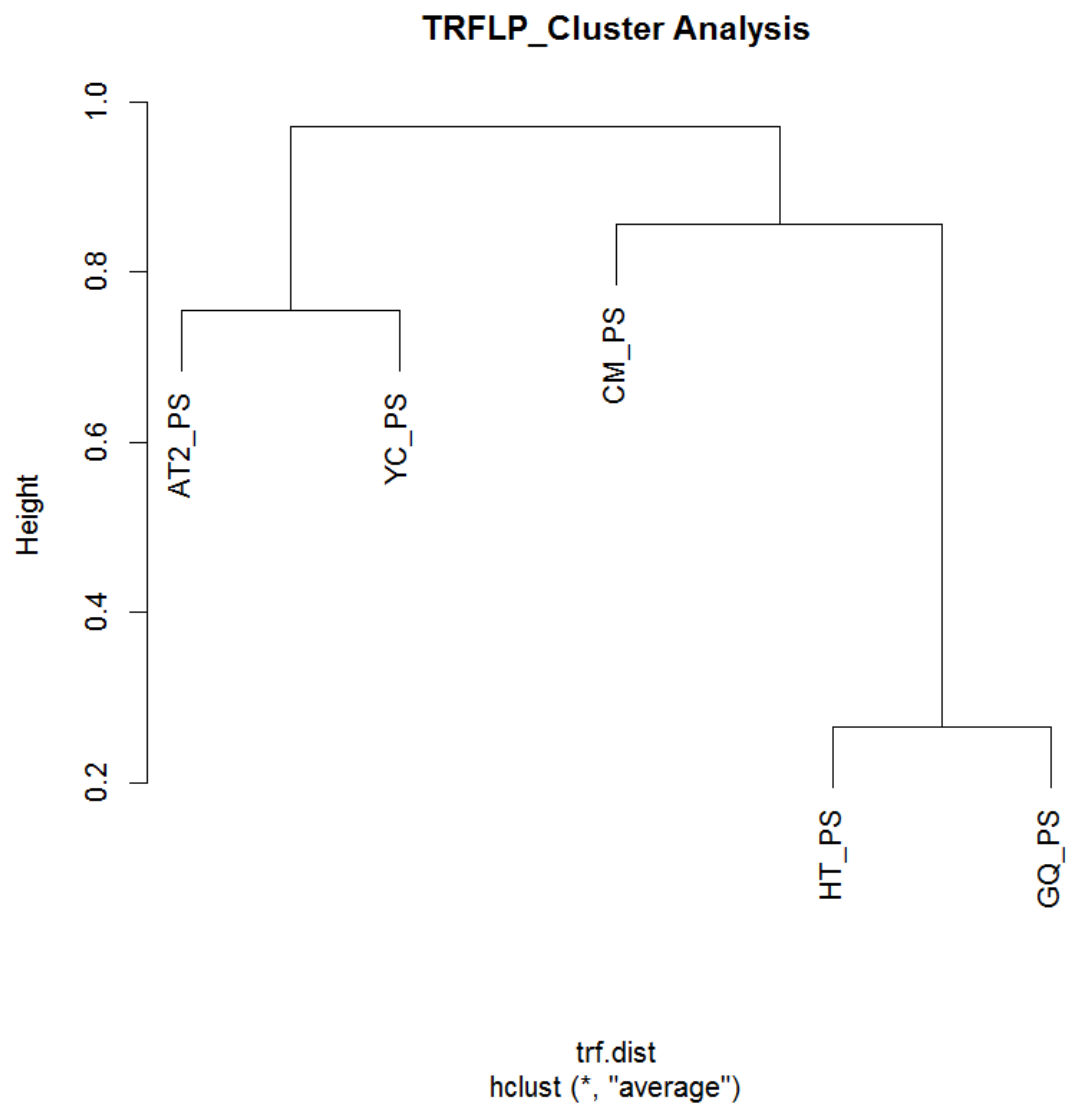


**Fig. 12:** Hierarchical clustering of samples from the from all travertine depositional facies. Analysis was based on the data from the T-RFLP profiles generated.

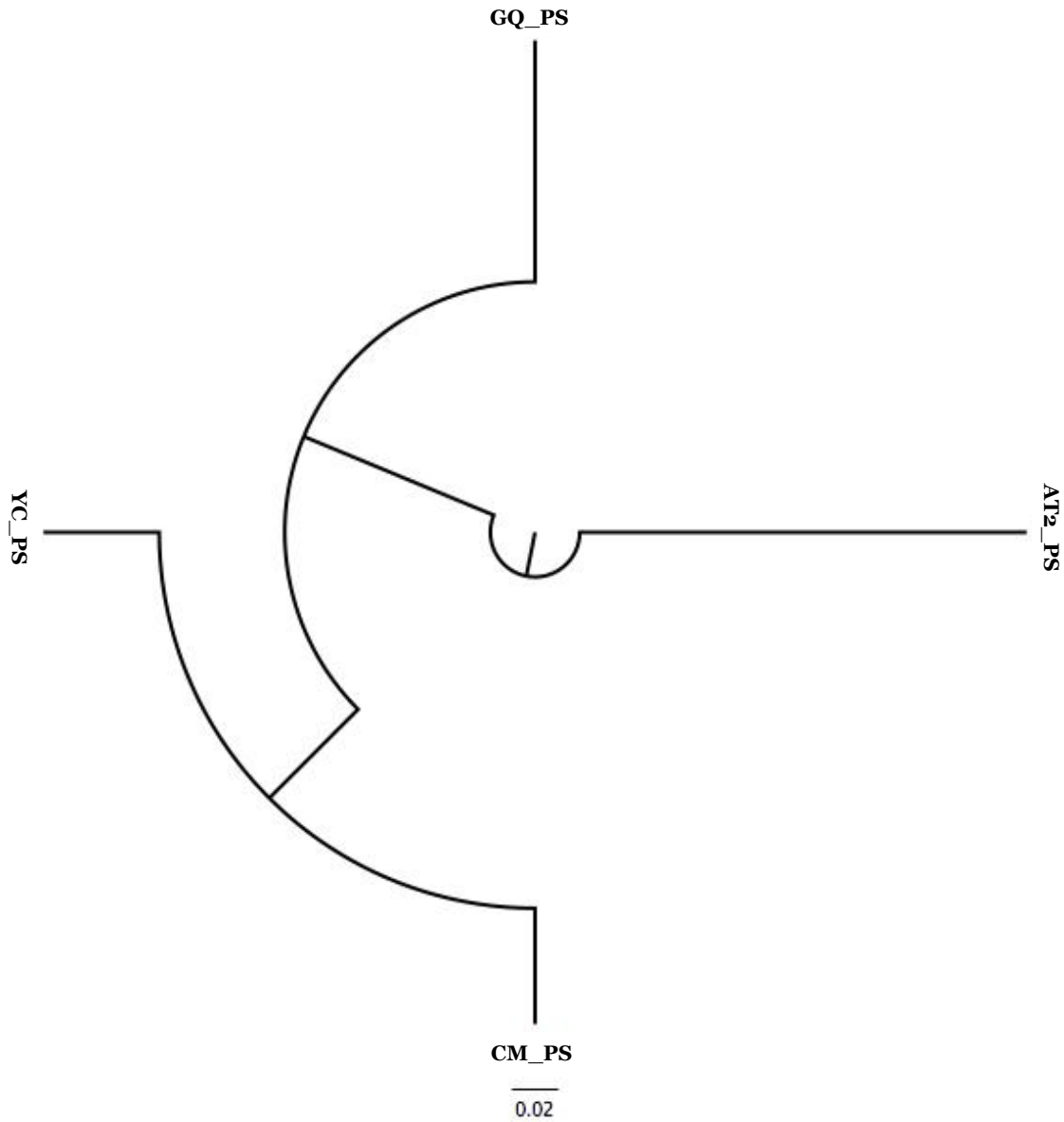


**Fig. 13:** Hierarchical clustering of samples from the from all travertine depositional facies. Analysis was based on the data from the 16S rRNA gene sequence librairies.

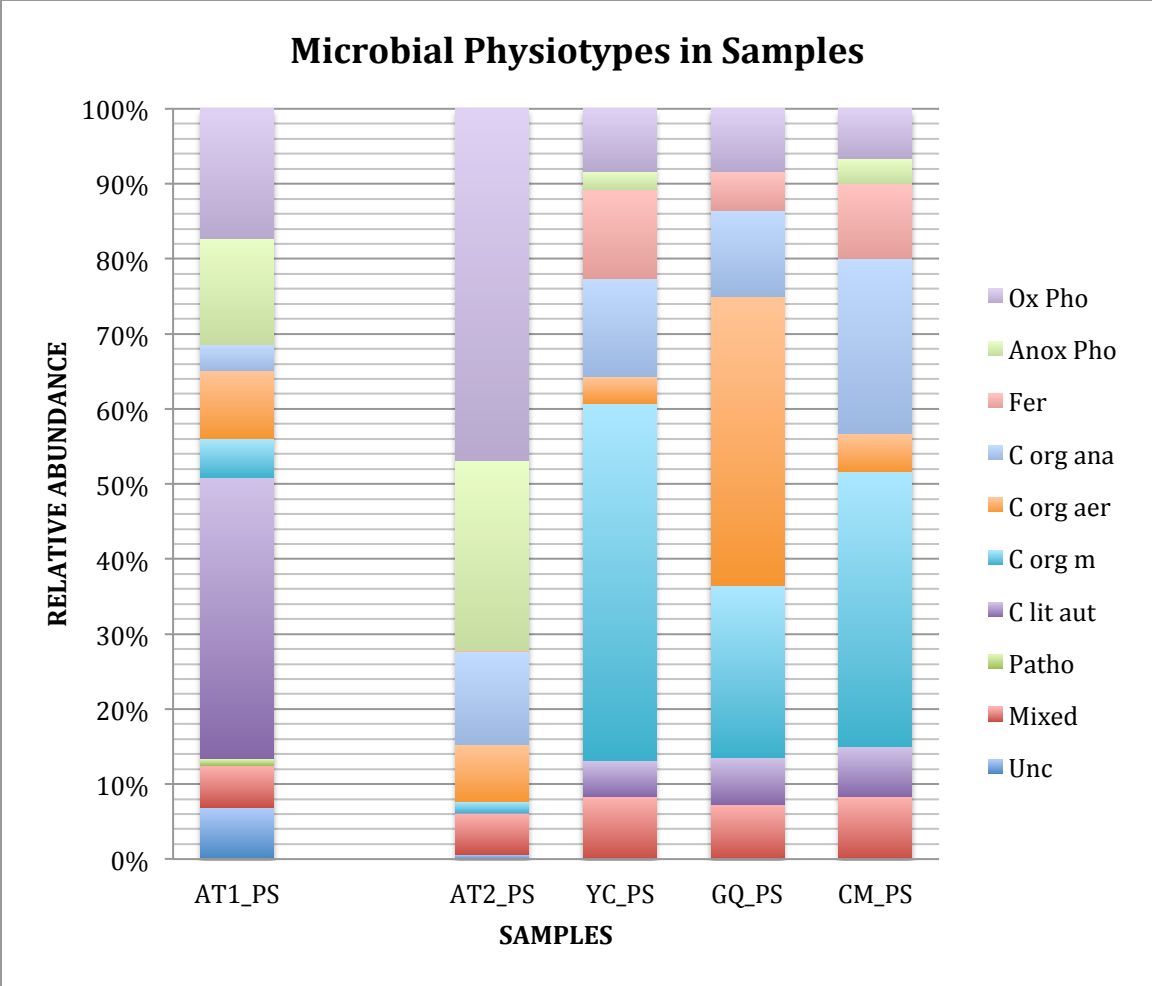


Fig. 14: A bar chart illustrating microbial physiotypes at the family level of identified gene sequences

**Table 1:** List of samples used in this study. All samples are from the Proximal Slope Facies

<b>NAME</b>	<b>LOCATION</b>	<b>AGE (YBP)</b>	<b>AGE</b>	<b>STUDY</b>
<b>AT1_PS</b>	AT1	0	Modern	Fouke et al., 2003
<b>AT2_PS</b>	AT2	~9	Modern	This study
<b>HT_PS</b>	NHT	~100	Recent Holocene	This study
<b>YC_PS</b>	Y-10 Core	~4000	Late Pleistocene	This study
<b>GQ_PS</b>	Gardiner	~30,000	Late Pleistocene	This study
<b>CM_PS</b>	Cakmak	~1.1 Ma	Middle Pleistocene	This study



**Table 2:** Genomic yield of samples of different ages. Ages were divided into 5 classes with 1 being the youngest samples and 5 being the oldest samples

<b>Sample Name</b>	<b>Concentration (ng/ul)</b>	<b>Age (years)</b>	<b>Age class</b>
<b>AT2_PS</b>	3.82	~9	1
<b>HT_PS</b>	0.548	~100	2
<b>YC_PS</b>	0.119	~4000	3
<b>GQ_PS</b>	0.092	~30,000	4
<b>CM_PS</b>	0.116	~1.1 Ma	5

**Table 3:** Sample specific barcodes for the samples investigated

<b>Sample ID</b>	<b>Barcode</b>
<b>AT2_PS</b>	TGCTACATCA
<b>HT_PS</b>	TCATATCGCG
<b>YC_PS</b>	TACGTATAGC
<b>GQ_PS</b>	TCGATGCGCT
<b>CM_PS</b>	TGATAGAGAG

**Table 4:** 16S rRNA gene sequencing results

<b>Sample ID</b>	<b>Original Number of Sequences</b>	<b>Quality Filtered Number of Sequences</b>	<b>Number of OTUs</b>
AT2_PS	133747	86698	354
HT_PS	17	12	0
YC_PS	53699	47609	50
GQ_PS	41347	34970	43
CM_PS	53389	48903	45

**Table 5:** 16S rRNA gene sequencing results for bacteria inhabiting sample AT1\_PS (Fouke et al., 2003)

<b>%ID</b>	<b>Best-Matched Organism</b>	<b>Acession #</b>	<b>Phylum</b>
98	<i>Sulfurihydrogenibium sp. YO3AOP1</i>	AF445739	Aquificales
99	<i>Sulfurihydrogenibium sp. YO3AOP2</i>	AF445734	Aquificales
85	<i>Flexibacter ruber</i>	AF445665	Bacteroidetes
83	<i>Roseivirga sp. F8</i>	AF445661	Bacteroidetes
85	<i>Adhaeribacter aquaticus</i>	AF445730	Bacteroidetes
86	<i>uncultured Flexibacter sp.</i>	AF445648	Bacteroidetes
87	<i>Candidatus Aquirestis calciphila</i>	AF445647	Bacteroidetes
98	<i>Algoriphagus alkaliphilus</i>	AF445684	Bacteroidetes
87	<i>Candidatus Aquirestis calciphila</i>	AF445660	Bacteroidetes
88	<i>Chlorobium limicola</i>	AF445662	Chlorobi
87	<i>Chlorobium limicola DSM 245</i>	AF446277	Chlorobi
87	<i>Chlorobium chlorochromatii CaD3</i>	AF446278	Chlorobi
87	<i>Chlorobium phaeobacteroides</i>	AF446279	Chlorobi
89	<i>Chloroherpeton thalassium ATCC 35110</i>	AF445706	Chlorobi
90	<i>Chloroherpeton thalassium ATCC 35111</i>	AF445663	Chlorobi
85	<i>uncultured Chlorobi bacterium</i>	AF445646	Chlorobi
99	<i>uncultured bacterium</i>	AF445709	Chlorobi
90	<i>Chloroherpeton thalassium ATCC 35110</i>	AF446337	Chlorobi
90	<i>Chloroherpeton thalassium ATCC 35111</i>	AF446338	Chlorobi
96	<i>uncultured bacterium</i>	AF445657	Chlorobi
86	<i>Chlorobium limicola DSM 245</i>	AF446276	Chlorobi
99	<i>uncultured Chloroflexi bacterium</i>	AF445672	Chloroflexi
99	<i>Roseiflexus sp. RS-1</i>	AF445666	Chloroflexi
99	<i>uc chloroflexi</i>	AF446251	Chloroflexi
98	<i>Uncultured Chloroflexus sp. clone YNP_SBC_MS3_B69</i>	AF446259	Chloroflexi
99	<i>Roseiflexus sp. RS-1</i>	AF445666	Chloroflexi
94	<i>uncultured bacterium</i>	AF445676	Chloroflexi
98	<i>uncultured Chloroflexus sp.</i>	AF445692	Chloroflexi
82	<i>Oscillatoria acuminata PCC 6304</i>	AF445744	Cyanobacteria
91	<i>Pseudanabaenoideae sp. Sai002</i>	AF446266	Cyanobacteria
98	<i>Spirulina sp.</i>	AF445678	Cyanobacteria
91	<i>Synechococcus elongatus CCMP1630</i>	AF446267	Cyanobacteria
99	<i>Synechococcus sp. C9</i>	AF445654	Cyanobacteria
99	<i>Synechococcus sp. JA-2-3B'a(2-13)</i>	AF446268	Cyanobacteria
94	<i>uncultured soil bacterium</i>	AF445677	Cyanobacteria
98	<i>Spirulina sp.</i>	AF445707	Cyanobacteria
99	<i>Synechococcus sp. JA-2-3B'a(2-13)</i>	AF445722	Cyanobacteria
99	<i>Juniperus virginiana chloroplast</i>	AF445656	Cyanobacteria
90	<i>Pseudanabaena limnetica CHAB792</i>	AF445691	Cyanobacteria

**Table 5 Cont'd**

<b>%ID</b>	<b>Best-Matched Organism</b>	<b>Acession #</b>	<b>Phylum</b>
93	<i>Microgenomates bacterium clone OPB92</i>	AF446256	OP 11
98	<i>Microgenomates</i>	AF445690	OP 11
99	<i>uncultured Microgenomates bacterium</i>	AF446252	OP 11
89	<i>Microgenomates bacterium clone OPB92</i>	AF446255	OP 11
94	<i>Microgenomates bacterium clone OPB92</i>	AF446323	OP 11
86	<i>iron-reducing bacterium enrichment culture clone HN122</i>	AF445645	Planctomyces
94	<i>uncultured bacterium</i>	AF446293	Proteobacteria
86	<i>Olavius ilvae associated proteobacterium Delta 8</i>	AF446295	Proteobacteria
98	<i>uncultured bacterium</i>	AF445733	Proteobacteria
89	<i>Gracilibacteria bacterium canine oral taxon 323</i>	AF445743	Proteobacteria
97	<i>Caulobacter sp. W2.09-217</i>	AF446301	Proteobacteria
90	<i>Caulobacter sp., strain FWC21</i>	AF446302	Proteobacteria
99	<i>Porphyrobacter sp. KK348</i>	AF445710	Proteobacteria
99	<i>Porphyrobacter sp. KK349</i>	AF445711	Proteobacteria
98	<i>Porphyrobacter donghaensis</i>	AF446308	Proteobacteria
94	<i>uncultured Hyphomonadaceae bacterium</i>	AF445674	Proteobacteria
87	<i>Dongia mobilis</i>	AF445655	Proteobacteria
96	<i>Brevundimonas sp. cf01</i>	AF445713	Proteobacteria
98	<i>Sphingomonas sp. GB1</i>	AF445712	Proteobacteria
89	<i>Rhodospirillum rubrum ATCC 11170</i>	AF445675	Proteobacteria
88	<i>Rhizobium sp. B2059</i>	AF445649	Proteobacteria
89	<i>Rhizobium sp. B2060</i>	AF445669	Proteobacteria
99	<i>uncultured bacterium</i>	AF445671	Proteobacteria
93	<i>uncultured bacterium</i>	AF445650	Proteobacteria
99	<i>uncultured delta proteobacterium</i>	AF446342	Proteobacteria
89	<i>Bdellovibrio bacteriovorus</i>	AF445705	Proteobacteria
100	<i>Brevundimonas bacteroides</i>	AF446300	Proteobacteria
94	<i>Rubribacterium polymorphum</i>	AF445668	Proteobacteria
94	<i>Hydrogenophilus hirschii</i>	AF446318	Proteobacteria
99	<i>Silanimonas sp. JK13</i>	AF446335	Proteobacteria
95	<i>Hydrogenophilus islandicus</i>	AF445689	Proteobacteria
90	<i>Leptospira borgpetersenii serovar Hardjo-bovis str. JB197</i>	AF445708	Spirochetes
84	<i>Thermus thermophilus HB8</i>	AF446258	Thermi
99	<i>Thermus thermophilus HB9</i>	AF445644	Thermi
97	<i>uncultured candidate division WS6 bacterium</i>	AF446332	WS6

**Table 6:** 16S rRNA gene sequencing results for bacteria inhabiting sample AT2\_PS

<b>ID %</b>	<b>Best-matched Organism</b>	<b>Accession #</b>	<b>Phylum</b>
100	Uncultured bacterium	JQ923511	Acidobacteria
94	<i>Solibacter usitatus</i> Ellin6076	NR_074351	Acidobacteria
100	Uncultured bacterium	FJ671296	Actinobacteria
100	Uncultured Micromonosporaceae bacterium	FM209146	Actinobacteria
99	<i>Jiangella alba</i>	NR_116547	Actinobacteria
98	<i>Sulfurihydrogenibium</i> sp. Y04ACSI	AF507961	Aquificae
99	<i>Pelodictyon phaeoclathratiforme</i> BU-1	NR_074365	Chlorobi
100	Uncultured Chlorobi bacterium	AF445653	Chlorobi
100	Uncultured Chlorobi bacterium	EF205464	Chlorobi
100	Uncultured Chlorobi group bacterium	AF445646	Chlorobi
91	<i>Thermanaerotherix daxensis</i>	NR_117865	Chloroflexi
100	Uncultured chloflexi bacterium	HQ190367	Chloroflexi
100	Uncultured bacterium	FJ886481	Chloroflexi
100	Uncultured Chloroflexi bacterium	AF445672	Chloroflexi
100	Uncultured bacterium	AF445731	Cyanobacteria
100	<i>Synechococcus</i> sp. TS-91	AY884060	Cyanobacteria
100	<i>Tolypothrix</i> sp. PCC 7504	FJ661003	Cyanobacteria
100	<i>Nodularia harveyana</i>	AF268019	Cyanobacteria
100	<i>Gloeotheca</i> sp. PCC 6909	HE975009	Cyanobacteria
100	Uncultured organism	JN432936	Cyanobacteria
91	<i>cyanobacterium</i> WH7B	AJ007374	Cyanobacteria
100	<i>Geitlerinema</i> sp. PCC 8501	FM210758	Cyanobacteria
100	<i>Pseudanabaena</i> sp. 1a-03	FR798944	Cyanobacteria
97	<i>Synechococcus</i> sp. C9	AF132773	Cyanobacteria
100	<i>Dictyoglomus turgidum</i> DSM 6724	CP001251	Dictyoglomi
100	<i>Bacillus</i> sp. Fen_H	JN247735	Firmicutes
99	<i>Bacillus subtilis</i>	JQ518358	Firmicutes
100	<i>Virgibacillus</i> sp. SCULCB PT-28	HQ620712	Firmicutes
100	<i>Paenibacillus favisporus</i>	EF173324	Firmicutes
99	<i>Chryseomicrobium</i> sp. AK52	HG529985	Firmicutes
99	<i>Planococcus rifietoensis</i>	KC842274	Firmicutes
99	<i>Exiguobacterium aurantiacum</i>	KJ722475	Firmicutes
99	<i>Trichococcus pasteurii</i> strain KoTa2	NR_036793	Firmicutes
100	Uncultured bacterium	EU454283	Firmicutes
98	<i>Clostridium</i> sp. JCC	HG726039	Firmicutes
100	<i>Clostridium</i> sp. Iso-W3	DQ677020	Firmicutes
99	<i>Sporacetigenium mesophilum</i>	NR_043101	Firmicutes
100	Uncultured bacterium	JX133375	Gemmatimonadetes
98	<i>Andersenella baltica</i>	NR_042626	Proteobacteria
99	<i>Rhodopseudomonas</i> sp. TUT3631	AB251406	Proteobacteria

**Table 6 Cont'd**

<b>ID %</b>	<b>Best-matched Organism</b>	<b>Accession #</b>	<b>Phylum</b>
99	Uncultured Devosia sp.	JN679184	Proteobacteria
100	<i>Paracoccus</i> sp. YT0095	AB362825	Proteobacteria
98	<i>Rhodobacter</i> sp. WS22	KF309179	Proteobacteria
100	<i>Candidatus Riegeria galatellae</i>	HQ689092	Proteobacteria
89	<i>Azospirillum</i> sp. 5C	AF413109	Proteobacteria
100	<i>Porphyrobacter donghaensis</i>	NR_025816	Proteobacteria
97	<i>Porphyrobacter</i> sp. KK351	AB033326	Proteobacteria
100	Uncultured Altererythrobacter sp.	EU530593	Proteobacteria
100	Uncultured bacterium	FJ382610	Proteobacteria
99	<i>Sphingomonas</i> sp. RHLT2-4	JX949369	Proteobacteria
99	<i>Porphyrobacter sanguineus</i>	AB062105	Proteobacteria
99	<i>Sphingomonas</i> sp. HX-H01	KF501484	Proteobacteria
100	<i>Sphingomonas</i> sp. MN6-10	JQ396564	Proteobacteria
100	<i>Sphingopyxis chilensis</i>	JF459974	Proteobacteria
100	<i>Beta proteobacterium</i> A40-2	AY049940	Proteobacteria
96	<i>Burkholderia</i> sp. enrichment culture clone CI5_3.5	GQ181151	Proteobacteria
97	<i>Burkholderia</i> sp. R4M-O	GQ478268	Proteobacteria
100	<i>Burkholderia</i> sp. Gc145	FJ528270	Proteobacteria
99	<i>Glacier bacterium</i> FJS22	AY315172	Proteobacteria
100	<i>Comamonas</i> sp. EB172	EU847238	Proteobacteria
99	<i>Hydrogenophaga</i> sp. 16-31G	KJ573531	Proteobacteria
99	<i>Albidiferax</i> sp. 7B-223	KF441665	Proteobacteria
97	<i>Tepidimonas thermarum</i>	AM042694	Proteobacteria
99	<i>Noviherbaspirillum</i> sp. THG-HS236	KF815075	Proteobacteria
100	<i>Paludibacterium</i> sp. HJ-DN4	JQ665441	Proteobacteria
100	Bacterium str. 51885	AF227840	Proteobacteria
95	<i>Hydrogenophilus islandicus</i>	NR_104511	Proteobacteria
97	Bacterium ROME95Asa	AY998140	Proteobacteria
100	<i>Sandaracinus amylolyticus</i>	NR_118001	Proteobacteria
97	<i>Nannocystis exedens</i> subsp. <i>cinnabaria</i>	KF267739	Proteobacteria
100	Uncultured delta proteobacterium	JF727693	Proteobacteria
100	<i>Escherichia coli</i> O124:H-	AB604196	Proteobacteria
100	<i>Escherichia coli</i>	CP010371	Proteobacteria
100	<i>Acinetobacter</i> sp. TS11	EU073077	Proteobacteria
99	<i>Pseudomonas poae</i> RE*1-1-14	NR_102514	Proteobacteria
100	<i>Stenotrophomonas</i> sp. OLI_1_4_SI	JF274783	Proteobacteria
99	<i>Stenotrophomonas</i> sp. ba7(2011)	JF772545	Proteobacteria
99	<i>Stenotrophomonas maltophilia</i>	JN705917	Proteobacteria
97	<i>Thermus arciformis</i>	NR_116251	Thermi

**Table 7:** 16S rRNA gene sequencing results for bacteria inhabiting sample YC\_PS

<b>ID %</b>	<b>Best-matched Organism</b>	<b>Accession #</b>	<b>Phylum</b>
100	<i>Cellulomonas sp. FFO16240</i>	AB023361	Actinobacteria
100	Uncultured Micromonosporaceae bacterium	FM209146	Actinobacteria
99	<i>Jiangella alba</i>	NR_116547	Actinobacteria
98	<i>Sulfurihydrogenibium sp. Y04ACSI</i>	AF507961	Aquificae
100	Uncultured bacterium	HM317227	Bacteroidetes
99	<i>Pelodictyon phaeoclathratiforme BU-1</i>	NR_074365	Chlorobi
100	Uncultured Chlorobi bacterium	EF205464	Chlorobi
100	<i>Geitlerinema sp. PCC 8501</i>	FM210758	Cyanobacteria
100	<i>Dictyoglomus turgidum DSM 6724</i>	CP001251	Dictyoglomi
100	<i>Bacillus sp. Fen_H</i>	JN247735	Firmicutes
99	<i>Bacillus subtilis</i>	JQ518358	Firmicutes
100	<i>Paenibacillus favisporus</i>	EF173324	Firmicutes
99	<i>Exiguobacterium aurantiacum</i>	KJ722475	Firmicutes
99	<i>Trichococcus pasteurii strain KoTa2</i>	NR_036793	Firmicutes
98	<i>Clostridium sp. JCC</i>	HG726039	Firmicutes
100	<i>Clostridium sp. Iso-W3</i>	DQ677020	Firmicutes
99	<i>Sporacetigenium mesophilum</i>	NR_043101	Firmicutes
97	<i>Porphyrobacter sp. KK351</i>	AB033326	Proteobacteria
100	<i>Schlegelella aquatica</i>	NR_043802	Proteobacteria
99	Glacier bacterium FJS22	AY315172	Proteobacteria
100	<i>Comamonas sp. EB172</i>	EU847238	Proteobacteria
99	<i>Polaromonas sp. GM1</i>	EU106605	Proteobacteria
97	<i>Tepidimonas thermarum</i>	AM042694	Proteobacteria
100	<i>Escherichia coli</i>	CP010371	Proteobacteria
100	<i>Acinetobacter sp. TS11</i>	EU073077	Proteobacteria
97	<i>Thermus arciformis</i>	NR_116251	Thermi



**Table 8:** 16S rRNA gene sequencing results for bacteria inhabiting sample GQ\_PS

<b>ID %</b>	<b>Best-matched Organism</b>	<b>Accession #</b>	<b>Phylum</b>
100	Uncultured actinobacterium	FN668231	Actinobacteria
100	Uncultured Micromonosporaceae bacterium	FM209146	Actinobacteria
98	<i>Sulfurihydrogenibium sp. Y04ACSI</i>	AF507961	Aquificae
83	<i>Thermomicrobium roseum</i>	M34115	Cyanobacteria
91	<i>Cyanobacterium WH7B</i>	AJ007374	Cyanobacteria
100	<i>Geitlerinema sp. PCC 8501</i>	FM210758	Cyanobacteria
100	<i>Dictyoglomus turgidum DSM 6724</i>	CP001251	Dictyoglomi
100	<i>Bacillus sp. Fen_H</i>	JN247735	Firmicutes
99	<i>Bacillus subtilis</i>	JQ518358	Firmicutes
100	<i>Paenibacillus favisporus</i>	EF173324	Firmicutes
99	<i>Planococcus rifietoensis</i>	KC842274	Firmicutes
99	<i>Trichococcus pasteurii strain KoTa2</i>	NR_036793	Firmicutes
100	<i>Clostridium intestinale</i>	AY781385	Firmicutes
100	<i>Clostridium sp. Iso-W3</i>	DQ677020	Firmicutes
99	<i>Sporacetigenium mesophilum</i>	NR_043101	Firmicutes
100	<i>Schlegelella aquatica</i>	NR_043802	Proteobacteria
99	<i>Albidiferax sp. 7B-223</i>	KF441665	Proteobacteria
97	<i>Tepidimonas therrmarum</i>	AM042694	Proteobacteria
95	<i>Hydrogenophilus islandicus</i>	NR_104511	Proteobacteria
100	<i>Escherichia coli O124:H-</i>	AB604196	Proteobacteria
100	<i>Escherichia coli</i>	CP010371	Proteobacteria
97	<i>Thermus arciformis</i>	NR_116251	Thermi

**Table 9:** 16S rRNA gene sequencing results for bacteria inhabiting sample CM\_PS

<b>ID %</b>	<b>Best-matched Organism</b>	<b>Accession #</b>	<b>Phylum</b>
99	<i>Nocardioides sp. V4.BE.17</i>	AJ244657	Actinobacteria
100	Uncultured Micromonosporaceae bacterium	FM209146	Actinobacteria
98	<i>Sulfurihydrogenibium sp. Y04ACSI</i>	AF507961	Aquificae
97	<i>Flavobacterium sp. R-40838</i>	FR682718	Bacteroidetes
100	Uncultured Chlorobi bacterium	EF205464	Chlorobi
100	<i>Geitlerinema sp. PCC 8501</i>	FM210758	Cyanobacteria
100	<i>Thermotogales str. SRI-15</i>	AF255594	EM3
100	<i>Bacillus sp. Fen_H</i>	JN247735	Firmicutes
99	<i>Bacillus subtilis</i>	JQ518358	Firmicutes
100	<i>Paenibacillus favisporus</i>	EF173324	Firmicutes
100	<i>Staphylococcus haemolyticus</i>	HG941667	Firmicutes
99	<i>Exiguobacterium aurantiacum</i>	KJ722475	Firmicutes
99	<i>Trichococcus pasteurii strain KoTa2</i>	NR_036793	Firmicutes
99	<i>Lactobacillus crispatus</i>	AB911459	Firmicutes
98	<i>Clostridium sp. JCC</i>	HG726039	Firmicutes
100	<i>Clostridium intestinale</i>	AY781385	Firmicutes
100	<i>Clostridium sp. Iso-W3</i>	DQ677020	Firmicutes
100	<i>Paracoccus sp. YT0095</i>	AB362825	Proteobacteria
99	<i>Hydrogenophaga sp. 16-31G</i>	KJ573531	Proteobacteria
99	<i>Albidiferax sp. 7B-223</i>	KF441665	Proteobacteria
97	<i>Tepidimonas therrmarum</i>	AM042694	Proteobacteria
98	<i>Geobacter sp. Ply1</i>	EF527233	Proteobacteria
100	<i>Escherichia coli</i>	CP010371	Proteobacteria
100	<i>Acinetobacter sp. TS11</i>	EU073077	Proteobacteria
100	<i>Fervidobacterium sp. CBS-2</i>	EF222229	Thermotogae
94	<i>Opitutus terrae PB90-1</i>	NR_074978	Verrucomicrobia

## REFERENCES

1. Aislabie J.K., Chhour D.J., Saul S., Miyauchi J., Ayton, R.F. Paetzold, and Balks, M.R. 2006. Dominant bacteria in soils of Marble Point and Wright Valley, Victoria Land, Antarctica. *Soil Biol. Biochem.* 38: 3041–3056.
2. Allen, C.C., Albert, F.G., Chafetz H.S., Combie, J. 2000. Microscopic physical biomarkers in carbonate hot springs: implications in the search for life on Mars. *Icarus* [Internet]. Available from: <http://www.sciencedirect.com/science/article/pii/S0019103500964352>
3. Allen, E.T., and Day, A.L. 1935. Hot springs of the Yellowstone National Park. Carnegie Institution of Washington Publication 466.
4. Antibus, D. E., L. G. Leff, B. L. Hall, J. L. Baeseman, and C. B. Blackwood. 2012. Cultivable bacteria from ancient algal mats from the McMurdo Dry Valleys, Antarctica. *Extremophiles* 16: 105–114.
5. Arbouille, D., Andrus, V., Piperi, T., and Xu, T. 2013. Sub-salt and pre-salt plays - How much are left to be discovered?: AAPG Search and Discovery Article no. 10545, adapted from a poster presentation given at AAPG International Conference and Exhibition, Cartagena, Colombia, 7 p, accessed December 15, 2014, [http://www.searchanddiscovery.com/pdfz/documents/2013/10545arbouille/ndx\\_arbouille.pdf.html](http://www.searchanddiscovery.com/pdfz/documents/2013/10545arbouille/ndx_arbouille.pdf.html)
6. Bargar K. E. (1978) Geology and thermal history of Mammoth Hot Springs Yellowstone National Park, Wyoming. *U. S. Geol. Surv. Bull.* 144.
7. Bernardet, J.F., Nakagawa, Y., Holmes, B. 2002. Proposed minimal standard describing new taxa of the family Flavobacteriaceae and emended description of the family. *Int J Syst Evol Microbiol* 52: 1049–1070
8. Blackwood, C. B., D. Hudleston, D. R. Zak, and J. S. Buyer (2007), Interpreting ecological diversity indices applied to terminal restriction fragment length polymorphism data: Insights from simulated microbial communities, *Appl. Environ. Microbiol.*, 73, 5276– 5283, doi:10.1128/AEM.00514-07.
9. Bonheyo, G.T., Frias-Lopez, J. and Fouke, B.W. 2005. A test for airborne dispersal of thermophilic bacteria from hot springs. In: *Geothermal Biology and Geochemistry in*

Yellowstone National Park. Proceedings of the Thermal Biology Institute Workshop, Yellowstone National Park, WY (Eds W.P. Inskeep and T.R. McDermott), pp. 327–342. Montana State University Press, Bozeman.

10. Borsodi E. 2014. 33 The Family Nocardioidaceae. Available from: [http://link.springer.com/content/pdf/10.1007/978-3-642-30138-4\\_193.pdf](http://link.springer.com/content/pdf/10.1007/978-3-642-30138-4_193.pdf)
11. Brock, T.D., Madigan, M.T., Martinko, J.M., and Parker, J. 2001. Biology of microorganisms. Prentice Hall, Upper Saddle River, N.J.
12. Butler, S.K., 2007. A facies-constrained model of Pleistocene travertine deposition and glaciation in the northern Yellowstone region. University of Illinois at Urbana-Champaign, MSc Thesis.
13. Canganella, F, and J Wiegel. 2014. Anaerobic Thermophiles. *Life*. Available at: <http://www.mdpi.com/2075-1729/4/1/77/html>
14. Carminatti, M., B. Wolf, and L. Gamboa, 2008. New exploratory frontiers in Brazil (abs.): 19th World Petroleum Congress, Madrid, June 29–July 3, 1 p.
15. Casanova, J. 1986. East African rift stromatolites. In Sedimentation in the African Rifts (ed. L. E. Frostick, R. W. Renaut, I. Reid and J. J. Tiercelin), pp. 201-10. Geological Society of London Special Publication No. 25.
16. Chafetz, H.S. and Folk, R.L. 1984. Travertines: depositional morphology and the bacterially constructed constituents. *J. Sediment. Petrol.*, 54, 289–386.
17. Claes, H., Soete, J., Van Noten, K., El Desouky, H., Erthal, M.M., Vanahecke, F. Ozkul, M., Swennen, R., n.d. Sedimentology, 3D geobody reconstruction and CO<sub>2</sub>-source delineation of travertine palaeo-deposits in the Ballik area. *Sedimentology*
18. DeSantis, T.Z., Hugenholtz, P., Larsen, N. 2006. Greengenes, a chimera-checked 16S rRNA gene database and workbench compatible with ARB. *Appl Environ Microbiol* 72(7): 5069-5072.
19. DeSantis, T.Z, Jr., Hugenholtz, P., Keller, K. 2006. NAST: a multiple sequence alignment server for comparative analysis of 16S rRNA genes. *Nucleic Acids Res* 34:394-399.
20. Dunbar, J., L. O. Ticknor, and C. R. Kuske (2000), Assessment of microbial diversity in four southwestern United States soils by 16S rRNA gene terminal restriction fragment

- analysis, *Appl. Environ. Microbiol.*, 66, 2943– 2950, doi:10.1128/AEM.66.7.2943-2950.2000.
21. Edgar, R.C. 2010. Search and clustering orders of magnitude faster than BLAST. *Bioinformatics* 26(19): 2460-2461.
  22. Fouke, B.W., Farmer, J.D., Marais, D.D., Pratt, L. 2000. Depositional facies and aqueous-solid geochemistry of travertine-depositing hot springs (Angel Terrace, Mammoth Hot Springs, Yellowstone National Park, USA). *Journal of Sedimentary ...* Available at: <http://jsedres.sepmonline.org/content/70/3/565.short>.
  23. Fouke, B.W. 2011. Hot-spring Systems Geobiology: abiotic and biotic influences on travertine formation at Mammoth Hot Springs, Yellowstone National Park, USA. *Sedimentology* 58.
  24. Fouke, B.W., Bonheyo, G.T., Sanzenbacher, B. and Frias-Lopez, J. 2003. Partitioning of bacterial communities between travertine depositional facies at Mammoth Hot Springs, Yellowstone National Park, U.S.A. *Canadian Journal of Earth Sciences* 40.
  25. Friedman, I. 1970. Some investigations of the deposition of travertine from hot springs— I. The isotopic chemistry of a travertine-depositing spring. *Geochimica et Cosmochimica Acta* .
  26. Gilichinsky DA, Wilson GS, Friedmann EI, McKay CP, Sletten RS, Rivkina EM, Vishnivetskaya TA, Erokhina LG, Ivanushkina NE, Kochkina GA, Shcherbakova VA, Soina VS, Spirina EV, Vorobyova EA, Fyodorov-Davydov DG, Hallet B, Ozerskaya SM, Sorokovikov VA, Laurinavichyus KS, Shatilovich AV, Chanton JP, Ostroumov VE, Tiedje JM. 2007. Microbial populations in Antarctic permafrost: Biodiversity, state, age, and implication for astrobiology. *Astrobiology* 7:275–311
  27. Golubic, S. 1973. The relationship between blue-green algae and carbonate deposits. In *The Biology of Blue-green Algae* (ed. N. G. Carr and B. A. Whitton), pp. 434-72. Oxford: Blackwells
  28. Golubic, S., and Focke, J. W. 1978. *Phormidium laminosum* Howe: identity and significance of a modern stromatolite-building microorganism. *Journal of Sedimentary Petrology* 48, 751-64.
  29. Guo, L., and Riding, R., 1994, Origin and diagenesis of Quaternary travertine shrub fabrics, Rapolanoi Terme, central Italy: *Sedimentology*, v. 41, p. 499-520.

30. Harris, A.G., Tuttle, E., Tuttle, S.D., 1997. *Geology of National Parks*, 5th edn. Kendall-Hunt Publishing, Dubuque, IA.
31. Hebsgaard, M. B., M. J. Phillips, and E. Willerslev. 2005. Geologically ancient DNA: fact or artefact? *Trends Microbiol.* 13: 212–20.
32. Jahnke L, Eder W, Huber R, Hope JM, Hinrichs K-U, Hayes JM, Des Marais DJ, Cady SL, Summons RE. 2001. Signature lipids and stable carbon isotope analyses of Octopus Spring hyperthermophilic communities compared with those of Aquificales representatives. *Applied and Environmental Microbiology* 67, 5179–5189.
33. Kandianis, M.T., Fouke, B.W., Veysey, J., Johnson, R.W. and Inskeep, W. 2008. Microbial biomass: a catalyst for CaCO<sub>3</sub> precipitation in advection-dominated transport regimes. *Geol. Soc. Am. Bull.*, 120, 442–450.
34. Kele, S., Ozkul, M., F.rizs, I., G.kg.z, A., Baykara, M.O., Al.i.ek, M.C., N.meth, T., Cihat, M., 2011. Stable isotope geochemical study of Pamukkale travertines: New evidences of low-temperature non-equilibrium calcite-water fractionation. *Sediment. Geol.* 238, 191–212. doi:10.1016/j.sedgeo.2011.04.015
35. Kennedy, M.J., Reader, S.L., and Swierczynski, L.M., 1994, Preservation records of microorganisms: evidence of the tenacity of life: *Microbiology*, v. 140, p. 2513-2529.
36. Knoll, A.H. (2003) *Life on a Young Planet: The First Three Billion Years of Evolution on Earth*. Princeton University Press, Princeton, NJ, 277 pp.
37. Lebatard, A.-E., Al.i.ek, M.C., Rochette, P., Khatib, S., Vialet, A., Boulbes, N., Bourl.s, D.L., Demory, F., Guipert, G., Mayda, S., Titov, V. V., Vidal, L., de Lumley, H., 2014. Dating the Homo erectus bearing travertine from Kocabaş (Denizli, Turkey) at at least 1.1 Ma. *Earth Planet. Sci. Lett.* 390, 8–18. doi:10.1016/j.epsl.2013.12.031
38. León, D. K., R Gerlach, and BM Peyton. 2013. Archaeal and bacterial communities in three alkaline hot springs in Heart Lake Geyser Basin, Yellowstone National Park. *Frontiers in Microbiology*
39. Lindahl T. 1993. Instability and decay of the primary structure of DNA. *Nature* [Internet] 362:709–15. Available from: <http://dx.doi.org/10.1038/362709a0>
40. Mann, S., 2001, *Biom mineralization: principles and concepts in Bioinorganic materials chemistry*: Oxford, Oxford University Press, 201 p

41. McDonald, D., Price, M.N., Goodrich, J., Nawrocki, E.P., DeSantis, T.Z., Probst, A., Andersen, G.L., Knight, R., Hugenholtz, P. 2012. An improved Greengenes taxonomy with explicit ranks for ecological and evolutionary analyses of bacteria and archaea. *ISME J* 6(3): 610–618.
42. McKay, D.S., Gibson, E.K., Thomas-Keptra, K.L., Vali, H., Romanek, C.S., Clemett, S.J., Chillier, X.D.F., Maechling, C.R., and Zare, R.N., 1996, Search for past life on Mars: possible relic biogenic activity in Martian meteorite ALH84001: *Science*, v. 273, p. 924-930.
43. Meyer-Dombard, DR, EL Shock, and JP Amend. 2005. Archaeal and bacterial communities in geochemically diverse hot springs of Yellowstone National Park, USA. *Geobiology*, 3: 211–227
44. Nakagawa, Y. 2011. Family I: Cytophagaceae. In: Krieg NR, Staley JT, Brown DR et al (eds) *Bergey's manual of systematic bacteriology*, vol 4. Springer, New York, pp 371–423
45. Nedashkovskaya, O.I., Kim, S.B., Hoste, B., Shin, D.S., Beleneva, I.A., Vancanneyt, M., Mikhailov, V.V. 2007a. *Echinicola vietnamensis* sp. nov., a member of the phylum Bacteroidetes isolated from seawater. *Int J Syst Evol Microbiol* 57:761–763
46. Osburn, M.R., LaRowe, D.E., and Momper, L.M. 2014. Chemolithotrophy in the continental deep subsurface: Sanford Underground Research Facility (SURF), USA. *Frontiers in Microbiology*
47. Osburn, M.R., Sessions, A.L. and Pepe-Ranney. C. 2011. Hydrogen-isotopic variability in fatty acids from Yellowstone National Park hot spring microbial communities. *Geochimica et Cosmochimica Acta* .
48. Oskam, C., Haile J., McLay, E., Rigby P., Allentoft, M., Olsen, M., Bengtsson, C., Miller, G., Schwenninger, J.-L., Jacomb C., et al. 2010. Fossil avian eggshell preserves ancient DNA. *Proceedings. Biological sciences / The Royal Society* [Internet], 277:1991–2000. Available from: <http://www.ncbi.nlm.nih.gov/pubmed/20219731>
49. Özkul, M., Varol, B., Alçiçek, M. 2002. Depositional environments and petrography of Denizli travertines. Available from: [http://www.mta.gov.tr/v2.0/eng/dergi\\_pdf/125/2.pdf](http://www.mta.gov.tr/v2.0/eng/dergi_pdf/125/2.pdf)
50. Özkul, M., Kele, S., Gökgöz, A., Shen, C.-C., Jones, B., Baykara, M.O., Fórizs, I., Németh, T., Chang, Y.-W. and Alçiçek, M.C. 2013. Comparison of the Quaternary

travertine sites in the Denizli extensional basin based on their depositional and geochemical data. *Sedimentary Geology* [Internet], 294. Available from: <http://dx.doi.org/10.1016/j.sedgeo.2013.05.018>

51. Paabo, S. 1989. Ancient DNA; extraction, characterization, molecular cloning and enzymatic amplification. *Proc. Natl Acad. Sci. USA* 86, 1939–1943.
52. Papineau, D, JJ Walker, and SJ Mojzsis. 2005. Composition and structure of microbial communities from stromatolites of Hamelin Pool in Shark Bay, Western Australia. *Applied And Environmental Microbiology*, Aug. 2005, p. 4822–4832
53. Pentecost A, Bauld J (1988) Nucleation of calcite on the sheaths of cyanobacteria using a simple diffusion cell. *Geomicrobiology Journal* Available at: <http://www.tandfonline.com/doi/abs/10.1080/01490458809377830>.
54. Pentecost, A (1990). The formation of travertine shrubs: Mammoth Hot springs, Wyoming. *Geological Magazine*.
55. Pentecost, A. (2005) *Travertine*. Springer-Verlag, Heidelberg, 445 pp.
56. Pentecost, A. 2003. Cyanobacteria associated with hot spring travertines. *Canadian Journal of Earth Sciences*.
57. Pentecost, A., S. Bayari, and C. Yesertener. 1997. Phototrophic microorganisms of the Pamukkale travertine, Turkey: their distribution and influence on travertine deposition. *Geomicrobiology Journal* 14: 269–283.
58. Pollack, J.B., Kasting, J.F., Richardson, S.M. and Poliakoff, K. 1987. The case for a wet, warm climate on early Mars. *Icarus*, 71, 203–224.
59. Russell, M.J. and Hall, A.J. 1997. The emergence of life from iron monosulphide bubbles at a submarine hydrothermal redox and pH front. *Journal of the Geological Society, London*, 154, 377–402.
60. Russell, M.J. and Hall A.J. 1999. On the inevitable emergence of life on Mars. In: Hiscox, J.A. (ed.) *The Search for Life on Mars. Proceedings of the First UK Conference*. British Interplanetary Society, 26–36.
61. Shi, T., Reeves, R.H., Gilichinsky, D.A., and Friedmann, E.I. 1997. Characterization of viable bacteria from Siberian permafrost by 16S rDNA sequencing. *Microb Ecol* 33: 169–179.



62. Skirnisdottir, S., Hreggvidsson, G.O., Hjorleifsdottir, S., Marteinson, V.T., Petursdottir, S.K., Holst, O., and Kristjansson, J.K. 2000. Influence of sulfide and temperature on species composition and community structure of hot spring microbial mats. *Applied and Environmental Microbiology*, 66: 2835–2841.
63. Sorey, M.L., 1991, Effects of potential geothermal development in the Corwin Springs known geothermal resources area, Montana, on the thermal features of Yellowstone National Park: Menlo Park, CA, United States Geological Survey.
64. Stackebrandt, E., Schumann, P. 2014. The Family Cellulomonadaceae. The Prokaryotes: Actinobacteria [Internet]. Available from: [http://link.springer.com/content/pdf/10.1007/978-3-642-30138-4\\_223.pdf](http://link.springer.com/content/pdf/10.1007/978-3-642-30138-4_223.pdf)
65. Stetter, K.O., Fiala, G., Huber, G., Huber, R. 1990. Hyperthermophilic microorganisms. *FEMS Microbiology* ... Available at: <http://onlinelibrary.wiley.com/doi/10.1111/j.1574-6968.1990.tb04089.x/abstract>.
66. Stetter, K.O. 1996. Hyperthermophilic procaryotes. *FEMS Microbiology Reviews*.
67. Steven, B., Briggs, G., McKay, C.P., Pollard, W.H., Greer, C.W., and Whyte, L.G., Characterization of the microbial diversity in a permafrost sample from the Canadian high arctic using culture-dependent and culture-independent methods, *FEMS Microbiol. Ecol.* 2007, vol. 59, pp. 513–523.
68. Sturchio, N.C., Murrell, M.T., Pierce, K.L., and Sorey, M.L., 1992, Yellowstone travertines: U-series ages and isotope ratios (C, O, Sr, U), in Kharaka, and Maest, eds., *Water-Rock Interaction: Rotterdam, Balkema*, p. 1427-1430.
69. Sturchio, N.C., Pierce, K.L., Murrell, M.T., and Sorey, M.L., 1994, Uranium-series ages of travertines and timing of the last glaciation in the northern Yellowstone area, Wyoming-Montana: *Quaternary Research*, v. 41, p. 265- 277.
70. Reysenbach, A.L., Ehringer, M., and Hershberger, K.L. 2000a. Microbial diversity at 83 °C in Calcite Springs, Yellowstone National Park: another environment where Aquificales and “Korarchaeota” coexist. *Extremophiles*, 4:61–67.
71. Reysenbach, A.L., Banta, A., Boone, D., Cary, S., and Luther, G. 2000b. Microbial essentials at hydrothermal vents. *Nature (London)*, 404: 835.
72. Takacs, C.D., Ehringer, M., Favre, R., Cermola, M., Eggertson, G., Palsdottir, A., and Reysenbach, A.L. 2002. Phylogenetic characterization of the blue green filamentous

- bacterial community from an Icelandic geothermal spring. *FEMS Microbiology and Ecology*, 35: 123–128.
73. Thomas-Keprta, K. L., D. A. Bazylinski, J. L. Kirchvink, S. J. Clemett, D. S. McKay, S. J. Wentworth, H. Vali, E. K. Gibson, Jr., and C. S. Romanek. 2000. Elongated prismatic magnetite crystals in ALH84001 carbonate globules: potential Martian magnetofossils. *Geochim. Cosmochim. Acta* 64:4049–4081.
74. Thomas-Keprta, K. L., S. J. Clemett, D. A. Bazylinski, J. L. Kirschvink, D. S. McKay, S. J. Wentworth, H. Vali, E. K. Gibson, Jr., M. F. McKay, and C. S. Romanek. 2001. Truncated hexa-octahedral magnetite crystals in ALH84001: presumptive biosignatures. *Proc. Natl. Acad. Sci. USA* 98:2164–2169.
75. Tunlid, A. and White, D.C. 1992. Biochemical analysis of biomass, community structure, nutritional status, and metabolic activity of microbial communities in soil. In: *Soil Biochemistry* (Bollag, J.M. and Stotzky, G., Eds.), pp. 229 – 262. Marcel Dekker, New York.
76. Van Noten, K., Claes, H., Soete, J., Foubert, A., Ozkul, M., Swennen, R., 2013. Fracture networks and strike–slip deformation along reactivated normal faults in Quaternary travertine deposits, Denizli Basin, western Turkey. *Tectonophysics* 588, 154–170. doi:10.1016/j.tecto.2012.12.018
77. Vorobyova E., Soina V., Gorlenko M., Minkovskaya N., Zalinova N., Mamukelashvili A., Gilichinsky D., Rivkina E. & Vishnivetskaya T. 2006. The deep cold biosphere: facts and hypothesis. *FEMS Microbiology Reviews* [Internet], 20: 270 – 290. Available from: <http://dx.doi.org/10.1111/j.1574-6976.1997.tb00314.x>
78. Vreeland, R. H. & Rosenzweig, W. D. 2002. The question of uniqueness of ancient bacteria. *J. Ind. Microbiol. Biotechnol.* 28, 32–41.
79. Vreeland R, Rosenzweig W, Lowenstein T, Satterfield C, Ventosa A. 2006. Fatty acid and DNA analyses of Permian bacteria isolated from ancient salt crystals reveal differences with their modern relatives. *Extremophiles: life under extreme conditions* [Internet] 10:71–8. Available from: <http://dx.doi.org/10.1007/s00792-005-0474-z>
80. Wang, Q., G. M. Garrity, J. M. Tiedje, and J. R. Cole. 2007. Naive Bayesian classifier for rapid assignment of rRNA sequences into the new bacterial taxonomy. *Appl Environ Microbiol* 73:5261-7.

81. White, D.E., Fournier, R.O., Muffler, L.J.P., and Truesdall, A.H. 1975. Physical results of research drilling in thermal areas of Yellowstone National Park, Wyoming. U.S. Geological Survey, Professional Paper 892.
82. Willerslev, E., Hansen, A. J. & Poinar, H. N. 2004b Isolation of nucleic acids and cultures from ice and permafrost. *Trends Ecol. Evol.* 19, 141–147.
83. Willerslev, E., and A. Cooper. 2005. Ancient DNA. *Proc. Biol. Sci.* 272: 3–16.
84. Woese C.R. 1987. Bacterial evolution. *Microbiological reviews*, p. 221-271
85. Zhang, C.L., Fouke, B.W., Bonheyo, G.T., White, D., Huang, Y. and Romanek, C.S. 2004. Lipid biomarkers and carbon isotopes of modern travertine deposits (Yellowstone National Park, USA): Implications for biogeochemical dynamics in hot-spring systems. *Geochim. Cosmochim. Acta*, 68, 3157–3169.